Hindawi Publishing Corporation
Journal of Sensors
Volume 2009, Article ID 861968, 20 pages
doi:10.1155/2009/861968

Review Article

Nanocrystalline Metal Oxides for Methane Sensors: Role of Noble Metals

S. Basu and P. K. Basu

IC Design and Fabrication Centre, Department of Electronic and Telecommunication Engineering, Jadavpur University, Kolkata 700032, India

Correspondence should be addressed to S. Basu, sukumar_basu@yahoo.co.uk

Received 1 January 2009; Revised 7 July 2009; Accepted 23 July 2009

Recommended by Giorgio Sberveglieri

Methane is an important gas for domestic and industrial applications and its source is mainly coalmines. Since methane is extremely inflammable in the coalmine atmosphere, it is essential to develop a reliable and relatively inexpensive chemical gas sensor to detect this inflammable gas below its explosion amount in air. The metal oxides have been proved to be potential materials for the development of commercial gas sensors. The functional properties of the metal oxide-based gas sensors can be improved not only by tailoring the crystal size of metal oxides but also by incorporating the noble metal catalyst on nanocrystalline metal oxide matrix. It was observed that the surface modification of nanocrystalline metal oxide thin films by noble metal sensitizers and the use of a noble metal catalytic contact as electrode reduce the operating temperatures appreciably and improve the sensing properties. This review article concentrates on the nanocrystalline metal oxide methane sensors and the role of noble metals on the sensing properties.

1. Introduction

Over the past 20 years, a great deal of research efforts has been directed towards the development of portable gas sensing devices for practical applications ranging from toxic gas detection to manufacturing process monitoring. For coalmines most of the accident occurs due to the presence of explosive and toxic gases like methane and carbon monoxide in air. In underground coalmines there are many kinds of ignition sources, such as electricity and frictions. Currently, it is suspected that a large roof fall may also act as the ignition source. This fall will compress air adiabatically and produce air temperature, well above the degree necessary to initiate a gas and/or coal dust explosion. So it is essential to monitor continuously the concentration of hazardous gases like CH_4 and CO and alarm if the gas concentration level is above a certain safety limit. Continuous research and development activities are being pursued to explore a gas sensor for detection of low concentrations of methane in the coalmine atmosphere at substantially low temperature so that the methane explosion is not further accelerated by the prevailing high temperature in the Mines [1, 2].

Semiconducting oxides are the fundamentals of smart devices as both the structure and morphology of these materials can be controlled precisely and so they are referred to as functional oxides. They have mainly two structural characteristics: cations with mixed valence states and anions with deficiencies. By varying either one or both of these characteristics, the electrical, optical, magnetic, and chemical properties can be tuned, giving the possibility of fabricating smart devices. The structures of functional oxides are very diverse and varied, and there are endless new phenomena and applications. Such unique characteristics make oxides one of the most diverse classes of materials, with properties covering almost all the aspects of materials science and in the areas of physics such as semiconductors, superconductivity, Ferro electricity, and magnetism.

Since the demonstration almost 50 years ago [3] that the adsorption of gas on the surface of a semiconductor can bring about a significant change in the electrical resistance

of the material, there has been a sustained and successful effort to make use of this change for the purposes of gas detection [4]. Sensing toxic and flammable gases is a subject of growing importance in both domestic and industrial environments. Metal oxides such as Ga_2O_3, SnO_2, WO_3, TiO_2, and ZnO [4–9] are stable physically and chemically and are widely investigated for gas and humidity detections. Sensing performance, especially response, is controlled by three independent factors: the receptor function, transducer function, and utility. Receptor function concerns the ability of the oxide surface to interact with the target gas. Chemical properties of the surface oxygen of the oxides are responsible for this interaction in an oxide-based device and this function can be largely modified. A considerable change in the response takes place when an additive (noble metal, acidic or basic oxide) is loaded on the oxide surface [8, 9]. Transducer function concerns the ability to convert the signal caused by chemical interaction of the oxide surface (work function change) into electrical signal. This function can be realized by the measure of the current through a system containing an innumerable number of grains and grain boundaries, to which a double-Schottky barrier model can be applied.

It has been observed by almost all researchers working with oxide semiconductors for gas sensing that the operation of such sensors with selectivity for a particular gas is extremely difficult, especially when the changes in the electrical properties are used as the sensor signal. Use of sensor arrays and artificial neural network can normally solve this problem. In fact today's chemical sensors are much more reliable with the implementation of ANN logic to improve the selectivity [10].

The objective of the present review is to discuss the role of noble catalyst metals to improve the functional properties of nanocrystalline oxide gas sensors for methane sensing.

2. Different Types of Semiconductor Metal Oxide Gas Sensors

Different structures of metal oxide gas sensors are innovated through research and development for the last few decades to improve the gas sensing performance. Some important structures are discussed in the following section.

2.1. Resistive Type Metal Oxide Gas Sensors. The first established and probably most well-known family of solid-state gas sensors comprises the resistive type metal oxide semiconductor sensors. This type of sensors are normally operated at temperature where the main contribution to variation of sensor signal originates from changes in the electronic conductivity due to charge transfer during chemisorptions and catalytic reactions at the surface and at grain boundaries. The advantage of this sort of sensors is the ease of fabrication and direct measurement capability. The resistance is measured between the two contacts taken from the top of the sensing (metal oxide) films deposited on a nonconducting substrates like glass [11], alumina [12], SiO_2 [13], and so forth.

2.2. Schottky Type Gas Sensors. The functional characteristics of sensors, for example, response magnitude and response time were improved over the resistive type sensors by adopting Schottky structures with catalytic metal electrode contacts as reported. Since most of the catalytic noble metals (Pd, Pt, Rh, etc.) make Schottky junctions with the semiconducting metal oxides and provide the catalytic effect as well as the collection of carriers, the metal layer serves as a gate for the diode. In presence of reducing gases, the hydrogen containing molecules suffers dissociative chemisorptions on metal electrode to produce atomic hydrogen. The atomic hydrogen diffuses into the metal/metal oxide junction and reduces the catalytic metal work function. The Schottky energy barrier changes due to the reduction of metal work function and this change can be measured by I-V, C-V, or any other electrical mode [14–16].

The double barrier Schottky junction in the metal-insulator-metal (MIM) configuration is another popular gas sensor device recently reported for hydrogen and methane sensing. Two different metals are deposited on either side of the oxide semiconductor to form back-to-back Schottky junctions. The advantage of such devices is that the total barrier is higher against the flow of free carriers. So, the current is appreciably low in air and the difference in current between the presence and absence of gas is quite high. Therefore, the response is high, and due to vertical transport of free carriers through the metal-semiconductor junctions the response time is also shorter compared to the planer sensor devices. The single Schottky barrier junction in MIM configuration is also superior to the planer devices in terms of response, response time, and recovery time. Basu and his research group reported hydrogen and methane sensing using ZnO MIM sensors [17, 18].

2.3. Metal Oxide Homojunction Gas Sensors. Normally metal oxides are *n*-type semiconductors. There are few metal oxides that also exhibit p-type conductivity such as CuO and NiO [19–21]. Recently p-type conductivity was reported in ZnO [19–21]. Thus the fabrication of semiconducting metal oxide p-n homojunction could be materialized with ZnO. Hazra and Basu [20, 21] showed that p-n ZnO homojunction is sensitive to H_2 as there is a substantial shift in the forward bias I-V characteristics on exposure to the reducing gases.

2.4. Metal Oxide Heterojunction Gas Sensors. Change in the I-V characteristics (on exposure to the gaseous environment) of heterojunction made of two dissimilar metal oxides with different band gap has evolved another new kind of gas sensor structures. Amongst these, ZnO/CuO is relatively widely explored one [22, 23] for sensing CO. Hu et al. [24] showed that ZnO/CuO also has good response towards H_2S and alcohol. The NO_2 and CO_2 sensing properties of a heterojunction gas sensor formed between *n*-type ZnO and a p-type composite based on a mixture of $BaTiO_3$/CuO/La_2O_3 were evaluated by Ling et al. [25] It was found that the $BaTiO_3$/CuO/La_2O_3 sensors showed an increase in resistance when exposed to NO_2. When exposed to CO_2

the $BaTiO_3/CuO/La_2O_3$ sensor showed a small decrease in resistance.

2.5. Mixed Metal Oxide Gas Sensors. Mixed oxides have recently emerged as promising candidates for gas detection [26–30]. It has been realized that such systems may benefit from the combination of the best sensing properties of the pure components. Formation of mixed oxides leads to the modification of the electronic structure of the system. This includes the changes in the bulk as well as in the surface properties. Bulk electronic structure, the band gap, Fermi level position, transport properties, and so forth are affected mostly in the case of compounds and solid solutions. Surface properties are expected to be influenced by new boundaries between grains of different chemical compositions. It is anticipated that all these phenomena will contribute advantageously to the gas sensing mechanism. The use of mixed oxides in gas detection (especially NO_2, H_2, CO) has been tried successfully *with* the following systems: SnO_2-TiO_2, SnO_2-WO_3, and TiO_2-WO_3 [30–36].

3. Methane Sensing Mechanism

It is well known that the performance of gas sensors can be improved by incorporation of noble metals on the oxide surface. SnO_2-based gas sensors in the form of thick film, porous pellets, or thin films, with Pt or Pd modifications, are widely applied for monitoring explosive and toxic gases in industry, urban and domestic life [37]. Such promoting effects are undoubtedly related to the catalytic activities of the noble metals for the oxidation of hydrocarbons. In case of planar type resistive gas sensors two metal contacts are taken from the metal oxide. A polycrystalline semiconductor has the structure with a large number of grains and grain boundaries. In contrast to the single crystalline materials, polycrystalline materials give rise to local potential barriers between the grains. The electrical properties of the surface of a thin film and the surface boundaries between the grains are affected by the adsorption and desorption of gaseous molecules. Oxygen ions can be found at the grain boundaries. At elevated temperature O_2 is chemisorbed by gaining [38, 39] one more electron from the surface. Due to this chemisorptions the resistivity of the material increases:

$$O + e^- \longleftrightarrow O^- \ [150^\circ C–300^\circ C], \tag{1}$$

$$2O + e^- \longleftrightarrow O_2^- [30^\circ C–150^\circ C]. \tag{2}$$

Methane molecules react with the chemisorbed oxygen at the grain boundaries. As a result negative charge carriers are added to the bulk and hence the resistance decreases:

$$CH4 + 4O^-_{(ads)} \longrightarrow CO_{2(air)} + 2H_2O + 4e^-_{(bulk)}. \tag{3}$$

Therefore, by measuring the change in the conductivity of the semiconductor oxide thin films we can detect the reducing gases [40].

In case of Schottky type gas sensors, catalytic noble metals are taken as the electrode contacts to the oxides. At an elevated temperature, the oxygen molecules are weakly bonded with the catalytic metal atoms (Pt, Pd-Ag, and Rh). The resulting complex subsequently dissociates and oxygen atoms are produced [41, 42]:

$$M + O_2 \longleftrightarrow 2Pd : O[M = Pd, Pt, Rh], \tag{4}$$

$$Pd : O \longleftrightarrow Pd + O. \tag{5}$$

The oxygen atoms then undergo a spillover process and finally form negatively charged surface ions by gaining electrons from the oxide surface, yielding a high electrostatic potential in the junction [43]. The space charge region, being depleted of electrons, is more resistive than the bulk. The hydrogen or methane response mechanism of gas sensors with a noble metal/metal oxide Schottky junction is, so far, the best understood and is illustrated in Figure 1. The first step is the dissociative adsorption of hydrogen or hydrogen containing molecules (like CH_4) to produce H or CH_3 on the noble metal surface that reacts with adsorbed atomic oxygen to produce water. Further, the H or CH_3 spillover to metal oxide surface and reacts with chemisorbed ionic oxygen to produce water and free electrons that increases the current through the junction. If the device is operated at an elevated temperature $\sim 100^\circ C$ or above, which is normally the case, the water molecules formed will rapidly desorb from the surface:

$$CH_4 \longrightarrow CH_{3(ads)} + H_{(ads)}, \tag{6}$$

$$CH_3 + H + 4O^- \longrightarrow CO_2 + 2H_2O + 4e^-, \tag{7}$$

$$CH_4 + 4O^- \longrightarrow CO_2 + 2H_2O + 4e^- (\text{Complete reaction}). \tag{8}$$

The above diagrams clearly demonstrate the methane sensing mechanism of noble metal/metal oxide Schottky junctions. While Figure 1(b) shows a change in capacitance with voltage in presence of gas, the same change can be recorded from I-V characteristics of the Schottky Junction where current is modulated in presence of detecting gas and thus there is a shift in the I-V curves. The energy band diagram of a typical Schottky junction is shown in Figure 2 and it clearly indicates that there is shift in band bending in presence of the sensing gas. As a result, the barrier height is modified and in fact for reducing gases like methane there is decrease in barrier height (n-ZnO) thereby allowing more current through the junction and thus increasing the conductivity.

Further due to its high solubility in catalytic metal and its rapid diffusion through the metal, hydrogen reaches the catalytic metal/metal oxide interface and produces an interfacial dipole layer as shown in Figure 1(c). The electrically polarized potential at the catalytic metal/metal oxide interface lowers the work function of catalytic metal and thus reduces the barrier height which is shown in the Energy Band Diagram (Figure 2). The hydrogen at the interface acts as a shallow donor to metal oxide (e.g., ZnO) and thus the barrier height is further reduced. Also, the adsorbed hydrogen atoms passivate the interface states between noble metal and metal oxide sensors, preventing them from charging and pinning

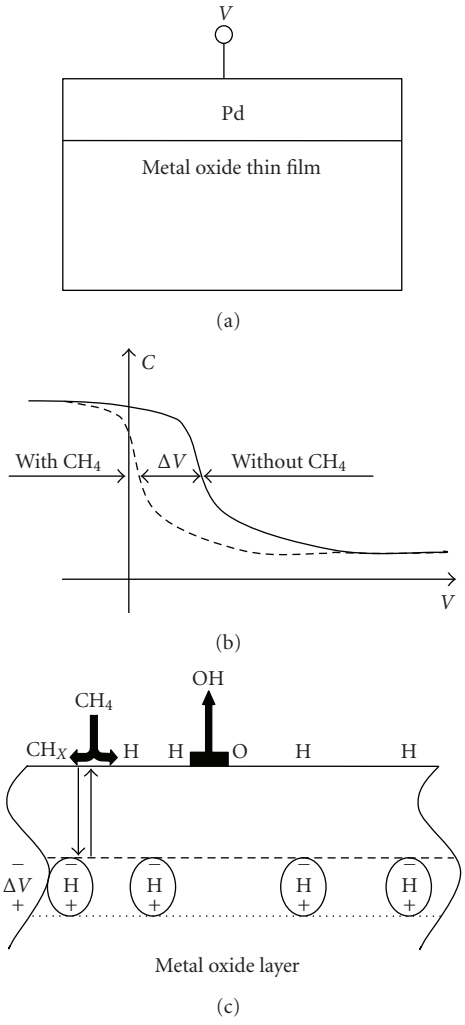

Figure 1: The schematic of hydrogen or methane sensing using catalytic metal on metal oxide film. (a) A typical noble metal/metal oxide Schottky junction. (b) When exposed to hydrogen or methane a voltage shift occurs in the capacitance—voltage characteristics. (c) Diffusion of hydrogen through the noble metal and formation of dipole layer across the noble metal/ metal oxide junction.

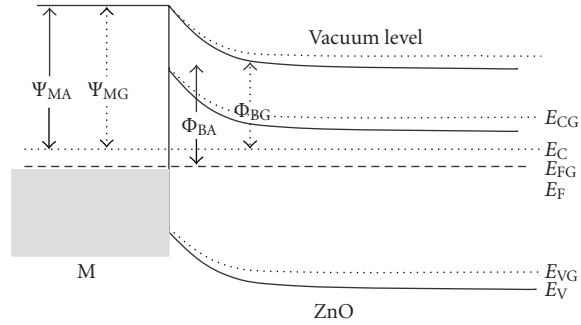

Figure 2: Band diagram of the Schottky Junction explaining the sensing mechanism. The barrier height reduces upon exposure to the reducing gas. ψ_{MA}, ψ_{MG} are the work function of M in air and in gas respectively. Φ_{BA}, Φ_{BG} are the barrier height of the junction in air and in gas, respectively. E_C, E_{CG} are the conduction band in air and in gas, respectively. E_V, E_{VG} are the valence band in air and in gas, respectively. E_F, F_{FG} are the fermi level in air and in gas, respectively. M is Pt, Pd, or Rh.

the fermi level. The passivated interface thus causes an improvement in the barrier height. Due to this lowering of barrier height, the current through the junction further increases in presence of the gas [5, 18, 44, 45], thereby yielding a high response.

4. Factors Related to the Improved Performance of a Gas Sensor

4.1. Grain Size Effect. Nano crystalline is a single phase or *a* multiphase of reduced size (1 nm to 100 nm) of at least one dimension. When the crystal size is decreasing, more and more surface is exposed. So fraction of atoms at the grain boundary increases and the grain boundaries contain a high density of defects like vacancies, dangling bonds, which can play an important role in the transport properties of electrons. Xu et al. [45] proposed a model to explain the dependence of depletion layer, due to adsorption of oxygen on the crystal size and to explain the high response of nanocrystalline metal oxide gas sensors. Later Rothschild and Komen [42] showed that the conductivity increases linearly with decreasing trapped charge densities and that the response to the gas-induced variations in the trapped charge density is proportional to $1/D$, where D is the average grain size. Figure 3 shows a schematic of few grains of nanocrystalline metal oxide thin films and the space charge region around the surface of each grain at the intergrain contacts. The space charge region, being depleted of electrons, is more resistive than the bulk. When the sensor is exposed to reducing gases, the electrons trapped by the oxygen adsorbate return to the oxide grains, leading to a decrease in the potential barrier height and thus the resistance drops. The crystallites in the gas sensing elements are connected to the neighboring crystallites either by grain boundary contacts or by necks. It was reported that [45] the higher response is obtained when grain size is much lower than twice the depletion width. The depletion region extends throughout the whole grains and the crystallites are almost fully depleted of electrons. As a result the conductivity decreases through the junction, and so the change of conductivity is very large in presence of reducing gases, thereby yielding a high response. Figure 3 demonstrates the three situations schematically.

Further, nanocrystalline metal oxides can reduce the operating temperature of the gas sensors. Zhang et al. [46] reported that the surface or interfacial tension decreases with decreasing particle size because of the increase in the potential energy of the bulk atoms of the particles. Smaller particles with increased molar free energy are more prone to adsorption per unit area of molecules or ions onto their surfaces in order to decrease the total free energy and to become more stable, and therefore, smaller particles have higher adsorption coefficient for gases. Thus, the adsorption

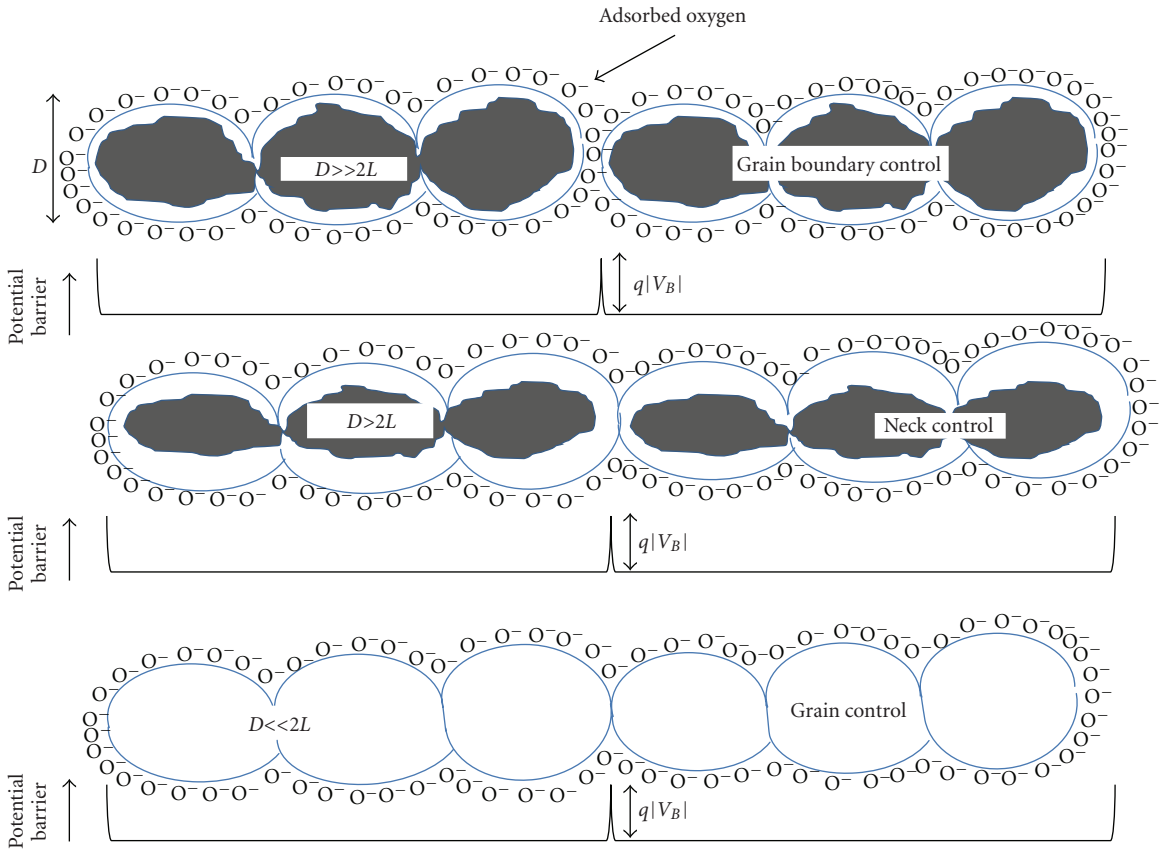

Figure 3: Schematic of few grains of nanocrystalline ZnO thin films and the space charge region around the surface of each grain at inter grain contacts.

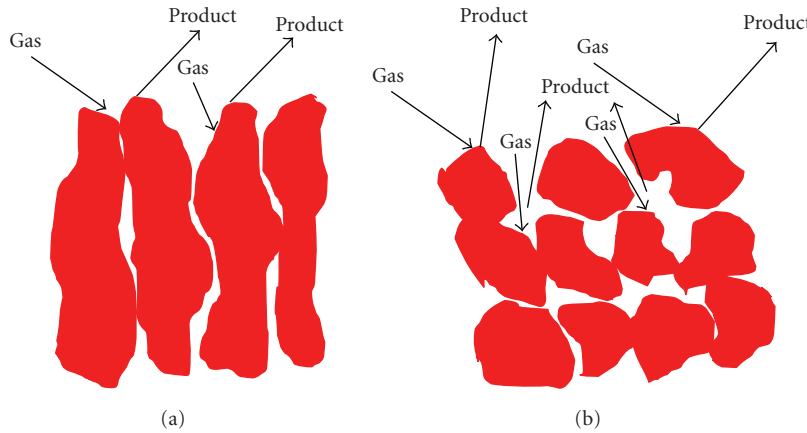

Figure 4: Schematic view of gas sensing reaction in (a) compact layer and (b) porous layer.

of oxygen or reducing gases takes place relatively easily onto the nano crystalline metal oxide surface.

4.2. Porosity and Thickness of the Metal Oxide Films. In compact metal oxide sensing layer, gases cannot penetrate into the layers and the gas sensing reaction is confined to the surface. In the porous layer, gases can access to the entire volume of the sensing layer and the gas sensing reaction can, therefore, take place at the surface of the individual grains, at the grain boundaries, and at the interface between grains and electrodes as shown in Figure 4. Therefore, porous layer is more suitable for methane sensing as compared to compact layers which has been already reported [18, 47–50].

The thickness of the metal oxide thin films has a great role to play on the response of the sensors. To get high response of the metal oxide-based gas sensors the thickness

of the electron-depleted region, due to the chemisorptions of oxygen, should be as close as the thickness of the metal oxide thin films. Generally, it was reported that the response is profoundly higher than resistive type gas sensors made of thinner films [51, 52]. Babaei and Orvatinia [53] proposed a model to establish a mathematical relation between the steady-state response of the sensor and the thickness of the sensitive film used. It was shown that the response drops exponentially as the thickness of the sensitive film increases. On the other hand, some groups reported that for certain combinations of the structural parameters like porosity, cracks, and so forth, the gas response of the sensors could increase.

4.3. Incorporation of Noble Metals. The performance of gas sensing can be improved by incorporation of noble metals into the metal oxides. SnO_2-based gas sensors in the form of thick film, porous pellets or thin films with the inclusion of Pt or Pd are widely applied for monitoring the explosive and toxic gases in industry, in urban, and domestic life. In fact, the catalytic metals do not change the free energy of the reactions but lower the activation energy. The noble metals can be incorporated as (i) electrode contact on metal oxide and/or (ii) dispersed phase on the oxide surface.

4.3.1. Effect of Noble Metal Electrode Contact on Metal Oxide. There are quite a few reports of the applications of nanoporous noble metal thin films as the electrode contact onto the metal oxides [54, 55]. Lofdahl et al. [56] studied the role of noble metal gate morphology for sensing hydrogen and some hydrocarbons. The metal gates were made with different thickness gradients. It was observed that Pd shows higher response at the thicker part of the film whereas Pt gives more or less the same response for both the thinner, and thicker part of the film. However, both Pd and Pt metal contacts show poor stability with time after repeated gas exposure. The Pd blistering at the thicker part of the metal film was also reported [57] for repeated hydrogen or hydrocarbon exposure. The change of response at the thicker, thinner and blistered part of the Pd film can be explained by water forming reaction. According to this report thick compact Pd layer is suitable for improved gas sensing.

The reduction of methane on Pd is not so simple as that of hydrogen. Recently Su et al. [58] proposed a mechanism of CH_4 reduction on Pd surface. They worked on ZrO_2 supported by Pd thin films. At an elevated temperature Pd is oxidized and then PdO is reduced in presence of methane. Very rapid oxidation occurs as a consequence of electric field-driven transport of oxygen anions through the oxide film. Once the film thickness exceeds about 15 nm, oxidation occurs more slowly via diffusive transport of oxygen through the oxide film. The reducing gases diffuse to the metal-oxide boundary where reduction of the oxide occurs. After the reduction of PdO continuous diffusion of H through Pd to Pd/metal oxide junction takes place and a dipole layer is formed. Dissociative adsorption of methane followed by water formation occurs almost simultaneously due to reaction of hydrogen with the chemisorbed oxygen.

There are some drawbacks associated with the use of pure Pd metal due to blister formation because of the irreversible transition from the α phase of palladium to the β hydride phase at low H_2 and at 300 K [59]. To overcome these problems Pd is alloyed to a second metal (13%–30% Ag) for H_2 or hydrocarbon sensing. Pd-Ag alloy is also attractive for use in gas sensors because of a numbers of other properties [60] reported as follows.

(1) The rate of hydride formation is very low for Pd-Ag alloy than for pure Pd.

(2) The solubility of hydrogen is actually greater up to about 30% Ag and the diffusion of hydrogen is not hindered by the Ag atom.

(3) Alloy at the higher Ag concentrations (up to 45%) was reported to have higher rates of hydrogen adsorption in the temperature range 30°C–100°C.

(4) The OH formation barrier energy is higher in presence of Pd-Ag alloy.

(5) The mechanical properties of polycrystalline Pd-Ag alloy are better than Pd.

4.3.2. Effect of Noble Metal Dispersion onto the Metal Oxide Surface. The gas response of the oxides is improved by surface modification by using platinum group metals like Pt, Pd, and Rh. These additives act as activators of the surface reactions. Generally, surface modification takes advantage of the following important options [61–63]:

(i) choosing a modifier that exhibits a catalytic activity in the solid-gas interactions,

(ii) changing the reactivity of the material by changing the modifier concentration,

(iii) the oxide semiconductor can affect the configuration of d electrons of surface-localized transition metals and change the surface activity by choosing a suitable "cluster-matrix" pair.

The most promising catalytic approaches are based on the "collective" and "local" site concepts. The "collective" site approach along with chemisorptions theory proposed by Volkenshtein [64] provides an idea of how the adsorbate affects the overall band structure of the modified matrix. It correlates the catalytic activity of the modifier directly to the valence state of the dopants in the oxide matrix and their influence on the charge carrier concentration in the semiconductor. On the other hand, the "local" sites approach is dealing with the concept of a nonuniform surface, which deals with the interaction of a semiconductor oxide with the gas phase to form a surface complex.

After noble metal deposition it is necessary to have subsequent annealing in the temperature range 300°C–600°C that improves the homogeneity and thus stabilizes the gas sensing properties [65]. The dispersed noble metals actually activate the spillover process as shown in Figure 5. Catalyst particles should be finely dispersed on the metal oxide matrix so that they are available near all the intergranular contacts. In an open atmosphere the oxygen molecules

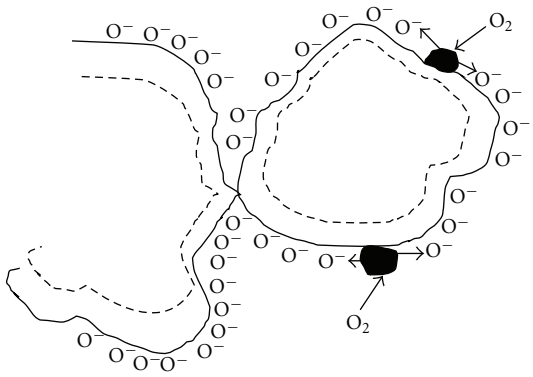

Figure 5: Oxygen spillover process in Pd modified ZnO thin films.

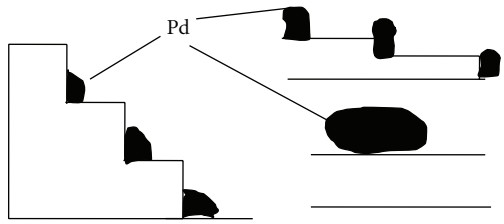

Figure 6: Nature of deposition of Pd modifier on the metal oxide matrix.

are first adsorbed on the catalyst and then spillover to the metal oxide matrix. At appropriate temperatures, the reducing gases are first adsorbed on to the surface of additive particles and then migrate to the oxide surface to react with surface oxygen species thereby increasing the surface conductivity. It was established that for attaining the optimal effect, surface cluster size should not exceed 1–5 nm [66], and the optimal distance between the clusters should be approximately equal to the oxygen surface diffusion length [67–69]. Recent experimental work has suggested that the noble metal clusters accumulate at the step edge of metal oxide (Figure 6). The functional parameters such as gas response, response time, recovery time, and selectivity have been dramatically improved through surface modification by noble metals. Further, the operating temperature can be shifted to lower value by introducing suitable noble metals.

5. Nanocrystalline Metal Oxide-Based Methane Sensors

Continuous research and development activities are being pursued to explore a gas sensor for detection of low concentrations of methane in the coalmine atmosphere at substantially low temperature so that the methane explosion is not further accelerated by the high sensing temperature. It has been realized that nanomaterials have great potential for the technological development almost in each area. The nanomaterials have some novel properties that attract for fundamental and technological research and development. The dots and wires in the nanoscale range develop the unique electrical and optical properties of materials. Quantum confinement effect due to the change of size and shape of the nanoparticles can modify the energy bands of the semiconductors and insulators. There are great efforts towards the development of nanostructured ZnO and SnO_2, since the reactions at the grain boundaries and a complete depletion of the carriers in the grains can strongly modify the material transport properties of metal oxide. The materials are characteristically *n*-type semiconductors due to nonstoichiometry associated with oxygen vacancy and/or metal excess in the interstices, acting as donor states to provide conduction electrons. However, the overall surface resistance of such films is greatly influenced by the chemisorptions of oxygen from air as discussed above.

5.1. Nanocrystalline SnO_2. Tin oxide (SnO_2) is an *n*-type semiconductor with a wide band gap ($Eg = 3.6$ eV). Because of its excellent optical and electrical properties, SnO_2 is extensively used as a functional material for the opto-electronic devices, gas sensors, varistor, ion sensitive field effect transistors, and transparent conductive coatings for organic light emitting diodes [70–73]. R.f. sputtering [74], dc-magnetron sputtering [75], thermal evaporation [76, 77], ion beam deposition [78], spray pyrolysis [79], and Sol-gel [80] are the most studied methods for the preparation of SnO_2. Sberveglieri [81] presented a review of the techniques applied for SnO_2 films deposition and it was shown that most of the methods require high-temperature treatments in order to fabricate good-quality polycrystalline films. High temperature, however, damages the surface of the films and increases the interface thickness, which has negative effect on the optical properties, especially on the wave guiding. Pulsed laser deposition (PLD) technique was successfully applied for growing quality SnO_2 thin films [82, 83]. The film was produced by ablation of either Sn target in oxidizing oxygen atmosphere or SnO_2 target. PLD offered many advantages of reduced contamination due to the use of laser light, control of the composition of deposited structure, and in situ doping. It is a versatile and powerful tool for production of nanoparticles with desired size and composition, only by varying the deposition conditions.

Carotta et al. [84] systematically studied the responses of alkanes to SnO_2-based materials and a solid solution of Sn, Ti with particular emphasis to the dehydrogenation mechanisms of surface reaction of these gases and eventually to carbon oxides. The mechanism of interaction of the sensors versus alkanes has been modelled on the basis of previously reported studies on oxidation of alkanes via heterogeneous catalysis of metal-oxide materials [85–87]. Also the sensing properties of SnO_2-and TiO_2-based oxides versus alkanes were studied [88] under wet condition and in presence of ethanol. It was observed that the response versus alkanes is significantly high, when operating above 450°C. In general, the response of the sensors versus alkanes increases with the number of carbon atoms and with temperature [89, 90]. This behavior is explained through alkane oxidation via heterogeneous catalysis of metal-oxide materials [85–87]. O-species at surface (oxygen adsorbed on the sensor surface)

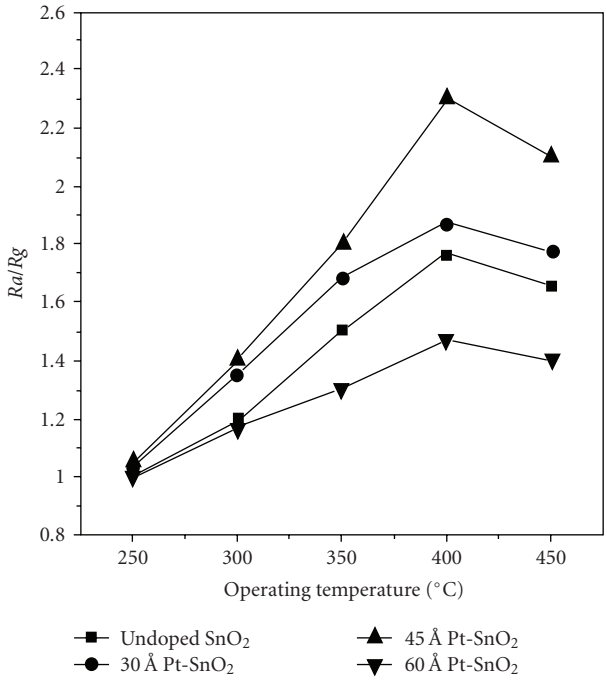

Figure 7: Response to 5000 ppm CH_4 as a function of operating temperature for undoped SnO_2 sensors with and without the Pt layers.

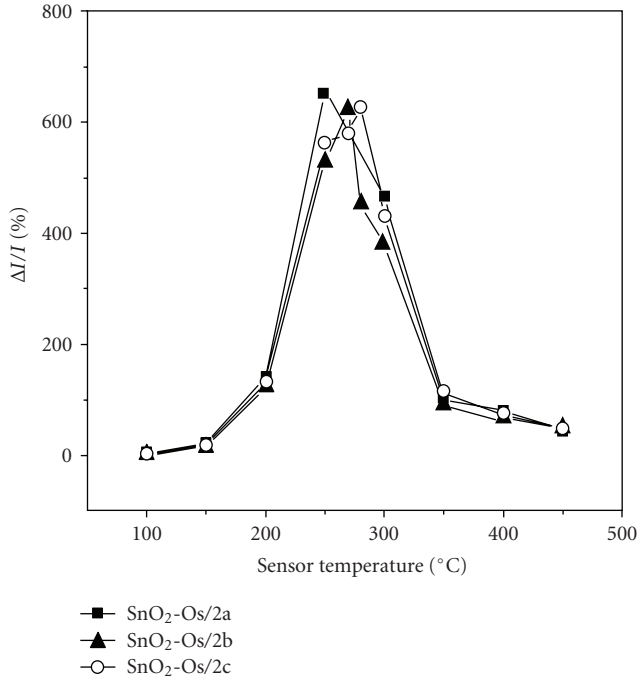

Figure 8: Response versus operating temperature for three Os-doped SnO_2 samples (2a, 2b, 2c are three SnO_2: Os samples doped with different Os concentrations).

trap hydrogen and an alkyl radical is being created. The radical reacts to give a second homolytic C–H bond dissociation and to form an alkene and a second OH–bond on the surface. Finally, the whole process yields an alkene, which then gets oxidized to CO, CO_2, and other subproducts The SnO_2 films were found suitable for this purpose at 650°C.

Recently Vaishampayan et al. [91]. studied the response of the pristine SnO_2 and Pd: SnO_2 towards different reducing gases. The 1.5 mol% Pd doping showed an enhancement in response to 75% and 95% towards LPG at as low a temperature as 50°C and 100°C, respectively, quite promising compared to pristine SnO_2. Structural characterizations revealed that Pd doping reduces the crystallite size of SnO_2 and helps in forming distinct spherical nanospheres at a calcination temperature of 500°C. Thus the increase in LPG response can be correlated with the spherical morphology and decrease in the crystallite size (11 nm) of SnO_2 due to doping with Pd as compared with the pristine SnO_2 (26 nm) and the role of Pd as a catalyst.

Cabot et al. studied [92] a correlation between the catalytic activity and the sensor response of different modified SnO_2 samples to CH_4 as target gas. It was found that the catalytic oxidation of methane is more pronounced for Pd than Pt. Recently Das et al. [93] observed that nanosized (3.5–14.0 nm) tin dioxide powders can be prepared by sonication-assisted precipitation. Thick films prepared by using such powders showed very good methane response because the resistance of the films in air at an operating temperature of 350°C was much less than that of the films prepared by conventionally precipitated powder. Also such sonication-assisted precipitated powder needs a lower amount of antimony doping for fabrication of real life gas sensors.

The undoped and 0.1 wt.% Ca-doped SnO_2 thin films were deposited by ion beam sputtering and were covered by 30–60 Å Pt layers that was annealed at 650°C. The methane sensors made of this film were tested in the temperature range 250–450°C. The best CH_4 response [94] was obtained at 400°C for a film with an optimal Pt thickness of45Å (Figure 7). Further it was found that the humidity dependence of CH_4 sensing up to 5000 ppm was relatively small because of the dense film structures.

Recently it was reported that Fe doped SnO_2 thick films also show response towards methane [95]. Quaranta et al. [96] studied the methane sensing properties of osmium-doped SnO_2 films that were prepared by Sol-gel technique using $SnCl_4$ and $OsCl_3$ precursors. The experimental data reported in this work show that Os doping improves the gas sensitive properties of the tin oxide thin films by enhancing the response to CH_4 and simultaneously by lowering the operating temperature that is shown in Figure 8. This is a promising work for producing a low-cost methane sensor. Probably, the role of Os is to act as a covalent site for catalyzing the oxidation of CH_4. Obviously, the reduction in the optimum operating temperature could lead to a cross-response effect, for example, response by CO. However, by using sensor in an array configuration, in which the interfering effects should not be a drawback, the problem of cross sensitivity may be solved. However, further studies are necessary to understand the true role of osmium in the catalytic property, reactivity, selectivity, and ageing effect in presence of interfering gases.

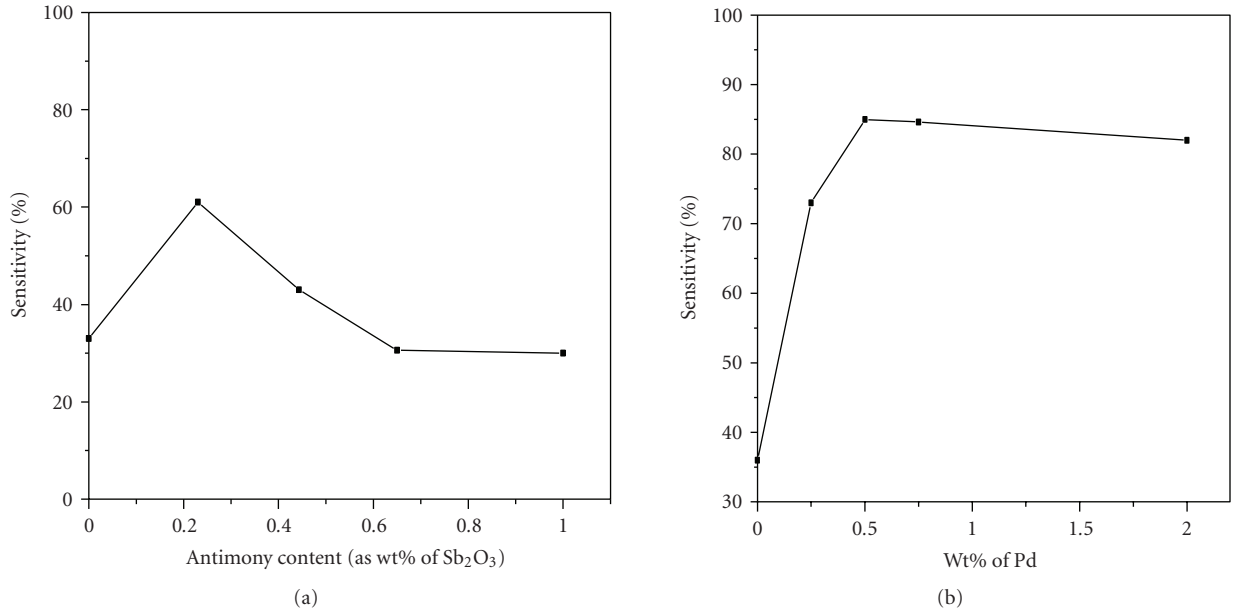

Figure 9: (a) Effect of antimony doping of tin dioxide on methane sensitivity and (b) effect of palladium concentration on methane sensitivity of tin dioxide.

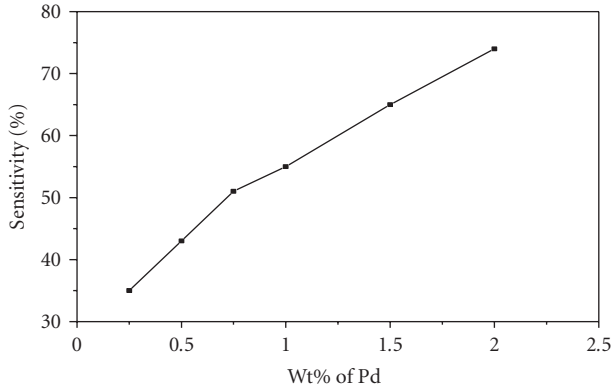

Figure 10: Effect of palladium concentration on methane sensitivity of antimony doped (0.5 wt.% as Sb_2O_3) tin dioxide coatings.

Chatterjee et al. [97] reported methane sensing characteristics of antimony-doped SnO_2 prepared by simultaneous precipitation of tin dioxide and antimony (0–1 wt.% as Sb_2O_3), tin dioxide and palladium (0–2 wt.% as Pd0), tin dioxide with a fixed amount of antimony (0.5 wt.% as Sb_2O_3) and palladium (0–2 wt.% as Pd0). Figures 9(a) and 9(b) demonstrate the dependence of methane sensitivity on antimony and palladium content in SnO_2 coating, respectively.

It was found that the antimony doping in small amounts gradually lowers the sensor resistance and there is an optimum antimony concentration (0.25%) where the response for methane is maximum (Figure 9(a))

The response of undoped tin dioxide for methane is maximum at 0.5 wt.% palladium (Figure 9(b)), but no such response saturation has been observed for palladium concentration up to 2 wt.% for antimony doped tin dioxide samples (Figure 10).

Kim et al. [98] prepared SnO_2 from $SnCl_4$ by a precipitation method using an aqueous ammonia solution of $SnCl_4$. The response of this sensor to methane at 658 K was higher than that with supported Pd, Pt, Rh, or Ni catalyst. This sensor responded to methane in the range 500–10,000 ppm with sufficiently high response and response rates, though it also responded to many other gases. Such an excellent promoting effect of the supported Pd (Figure 11) catalyst is considered to originate from the high dispersion of Pd (or PdO) particles supported in addition to the high intrinsic activity of Pd for the catalytic oxidation of methane.

Urfels et al. [99] reported that Pt supported on high surface area tin (IV) oxide appears as a superior catalyst for the complete oxidation of traces of methane at low temperature, being even significantly more active than reference Pd/Al_2O_3 in the presence of large amounts of water in the feed. This is due to the fact that the inhibition of water on the catalytic activity is not as strong as for Pd/Al_2O_3. Pt/SnO_2 [100] is however more severely deactivated than Pd/Al_2O_3 upon steam ageing at 873 K and that would predict a shorter lifetime compared to Pd catalysts [12]. The presence of H_2S induces a strong and irreversible deactivation of Pt/SnO_2. The activity is hardly restored by treatment under oxidizing atmosphere below 773 K due to the stability of poisoning species.

Chakraborty et al. reported [101] a thick film methane sensor that was fabricated from nanosized tin dioxide powder containing antimony oxide and palladium. Thick film sensors, prepared with such powders, showed good methane response and nearly equivalent sensing properties of imported Figaro (Japan) sensors. Han et al. [102] worked on SnO_2 based-gas sensors and it was found that Fe_2O_3

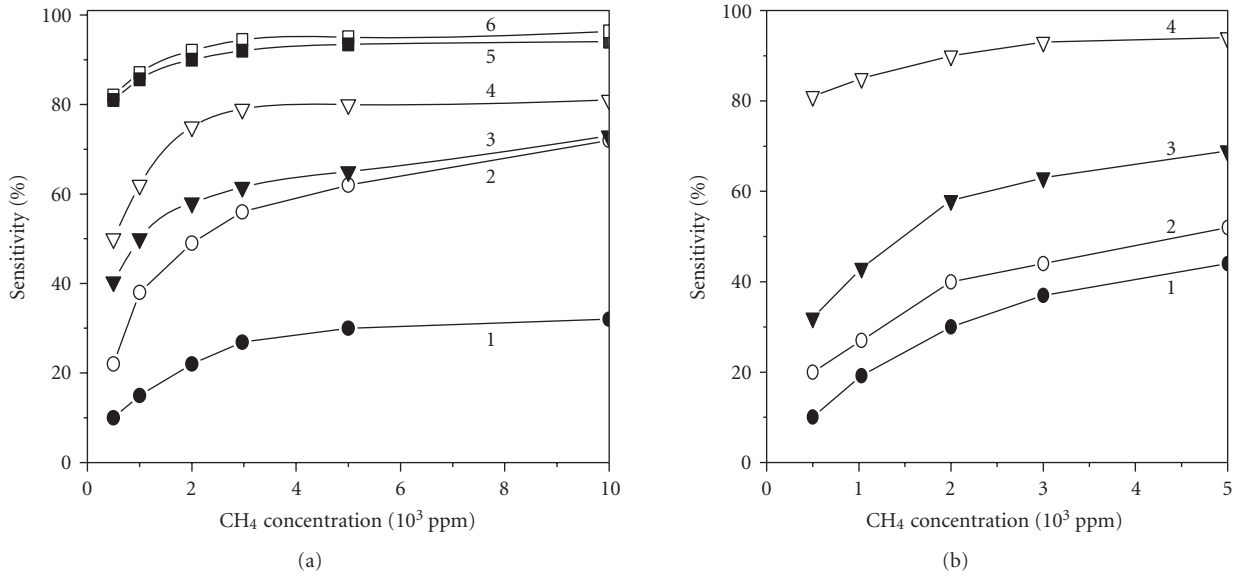

Figure 11: (a) The sensitivities of SnO_2-based sensors having various combinations of additivities (Ca and Pt) and alumina supported metal catalysts (Pd and Pt) to methane at 658 K as a function of methane concentration. The additivities (0.1 wt.%) were added to SnO_2 by a coprecipitation method, while the supported catalysts (5 wt.%) were mixed with SnO_2 powder. (1) SnO_2 (pure), (2) SnO_2 (Ca), (3) SnO_2 (Ca, Pt), (4) SnO_2 (pure) + Pt:alumina, (5) SnO_2 (pure) + Pd:alumina, and (6) SnO_2 (Ca,Pt) + Pd:alumina. (b) Influences of Pd loading methods on the methane sensitivities at 658 K (net Pd loading: 0.25 wt.%). (1) Impregnation from $PdCl_2$ solution. (2) Physical mixing of Pd black. (3) Rinsing method. (4) Physical mixing of Pd: alumina.

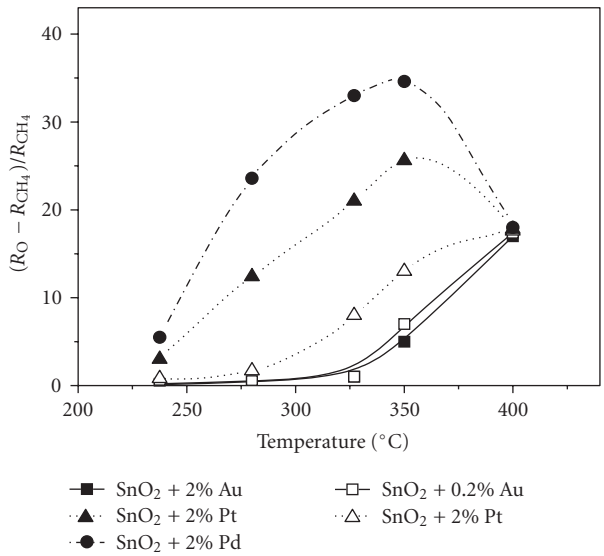

Figure 12: Sensor response to 1000 ppm CH_4 as a function of the operating temperature. Open symbols correspond to the SnO_2 materials with a nominal 0.2% additive concentration and black symbols correspond to those with 2% additive.

was a more effective additive than Pd or Pt. It showed high response and high selectivity for H_2, CH_4, and C_4H_{10} and a little cross-sensitivity to ethanol and smoke. Malyshev and Pislyakov and his group [103] developed a production process of thick-film semiconductor gas sensors. The sensors were proved to be highly efficient for detection of methane, hexane, hydrogen, carbon monoxide, ammonia, hydrogen sulphide, and ethanol. Saha et al. [104] studied the role of alumina on the methane response of the tin oxide thin films and a good response was observed. Above 350°C, in contrast to pure tin dioxide coatings, the methane response of iron doped tin dioxide coatings drastically decreased. The nanocomposites based on Sn, In, and Ti oxides were successfully derived by Chen et al. [105] with high response and selectivity for methane through optimizing the preparation parameters. Enhancement of gas-sensing properties of the semiconducting methane sensor could be attributed to the smaller crystallite size of SnO_2, the adsorption behavior and the chemical reaction of methane and O_2 on the composite surface, and to the introduction of the additives. The sensing behavior was directly related to the catalytic activity for methane oxidation.

5.2. Nanocrystalline ZnO. ZnO is a promising material for gas sensor. So far ZnO-based devices have attracted much attention as gas sensors because of their chemical response to different adsorbed gases, high chemical stability, amenability to doping, no toxicity, and low cost. ZnO gas sensors can be used not only for detecting the leakage of inflammable gases and toxic gases but also for controlling domestic gas boilers. Zinc oxide is a wide band gap semiconductor with many important properties, which make it commonly used in electronic and optoelectronic applications. Polycrystalline ZnO has been widely used in electronic industry. Pure ZnO is an intrinsic II-VI compound semiconductor with a band

gap of 3.2 eV at room temperature (30°C) and high exciton binding energy (60 meV). The nature of absorption shows that ZnO is a direct band gap semiconductor. The creation of native defects during preparation makes ZnO normally *n*-type [106–108]. The nonstoichiometry arises due to excess zinc interstitials or oxygen vacancies or both which make ZnO *n*-type semiconductor.

ZnO films can be prepared by many methods, such as thermal oxidation of Zn metallic films [109], sol gel process [110], sputtering [111], chemical vapor deposition [112], pulse laser deposition[113], evaporating method [114], and electrochemical process [115, 116].

For the last couple of years investigations on the development of a low-temperature methane detector using nanocrystalline ZnO-based chemical gas sensors with noble metals as the catalytic metal contacts have become quite important. The challenge is to attain the high response of low ppm testing gases, short response and recovery time, selectivity, and long-range stability. Nanocrystalline ZnO thin films demonstrate remarkable gas-sensing properties when the crystallite size becomes comparable to Debye length. Further, nanocrystalline and porous materials with controlled composition are of increasing interest in gas sensing because of their large surface to volume ratio that enhances the reaction probability between the adsorbed oxygen and methane gas.

Mitra and Mukhopadhyay [117] reported Methane (CH_4) response of zinc oxide (ZnO) thin film. The catalyst layer was formed on the surface of semiconducting ZnO following a wet chemical process from palladium chloride ($PdCl_2$) solution. A reasonable response of approximately 86%, fast response time of less than one minute, and a moderately fast recovery (approximately 3 minutes) are observed at 200°C. Although the operating temperature of 200°C is relatively on the lower side, the maximum response of 86% should be somewhat higher for application purpose.

Recently the methane sensing temperature between 210°C and 250°C is reported [118–120] depending upon whether the ZnO sensing film was grown electrochemically or by a sol-gel method**,** respectively. But these relatively high temperatures for detection of methane are still not suitable for applications in the coalmines**.**

The functional characteristics of the gas sensors, for example, response, response time, and recovery time were improved over the resistive Taguchi type sensors by adopting Schottky structures with catalytic metal contact. The vertical structure fabricated by growing metal oxides on the conducting surface and depositing a catalytic metal on the oxide improves the functional properties of the sensor devices because the electrons generated in the catalytic metal-oxide interface can be collected by the second electrode in the back with minimum carrier annihilation in the transport mechanism. Fonash [121] first studied the MIM configurations. The basic principle of the current conduction mechanism of an MIM sensor is that the electrons move from the upper metal electrode to the lower one through the active insulating layer vertically on the basis of back-to-back Schottky barrierjunctions. In the MIM configuration

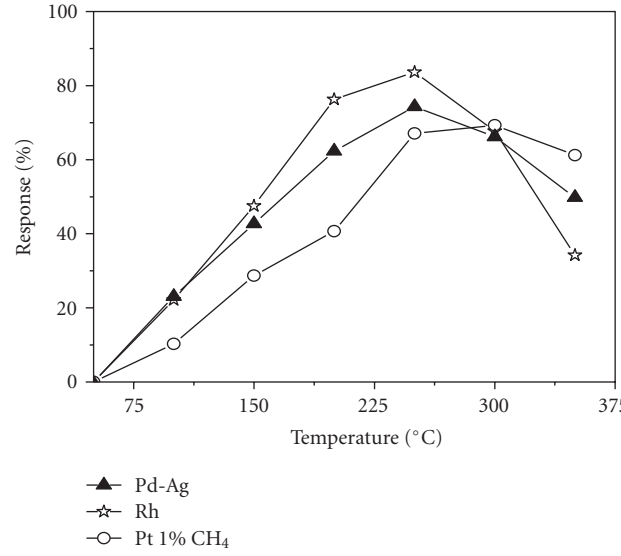

Figure 13: Response magnitude as a function of temperature for Pd-Ag, Rh, and Pt contacts.

since Zn contact to ZnO layer is ohmic by nature, only noble metal/ZnO junction acts as the barrier against electron flow. Room temperature hydrogen sensor using ZnO MIM structure was first reported by Dutta and Basu [122]. There are very few reports on Zinc oxide-based methane gas sensors with high response and faster response time and recovery time. So far the reported sensor structures on the oxide-based semiconductors and operating in the resistive mode at high temperatures showed longer response and recovery time [118–127].

Bhattacharyya et al. [120] studied the sol-gel grown ZnO-based gas sensors in the resistive mode. Pd-Ag and Rh contacts were found to produce a relatively lower optimum temperature of 250°C for sensing compared to 300°C for Pt contact. Further, Rh contact showed the higher response (83.6%) than Pd-Ag and Pt (Figure 13). It was further reported that the response and recovery time are shorter for Pd-Ag compared to Rh and Pt contacts, most probably due to the fact that solubility and diffusivity of hydrogen obtained from methane dissociation is higher for Pd-Ag compared to both Pt and Rh [128–131].

Basu et al. [126, 127] have studied electrochemically grown ZnO-based MIM Schottky gas sensors and the effect of different catalyst metals (Rh, Pt, and Pd-Ag) on methane sensing. The response versus temperature curves for different noble metal catalysts in pure nitrogen is shown in Figure 14 and it is observed that Rh gives higher response than Pd-Ag and Pt (Rh>Pd-Ag>Pt). In fact, the catalytic effect of Rh for dissociation of methane or hydrogen is stronger than Pd and Pt. In literature, it can be found that catalytic activity of Pd and Pt on methane or hydrogen is more or less the same [128–131]. But Figure 14 shows a higher response with Pd-Ag than Pt and thus contradicts the reported results. Figure 14(b) further shows that the response is somewhat reduced in synthetic air. It was reported that the oxygen is parallely chemisorbed on the noble metal and there is a

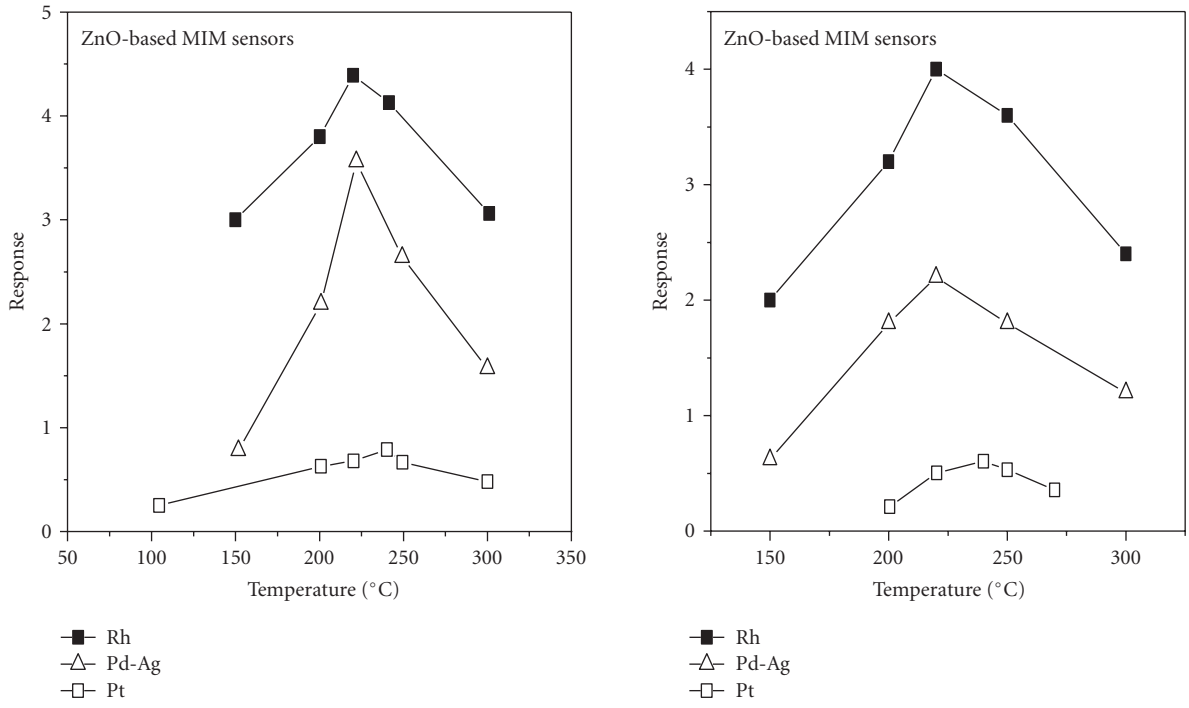

Figure 14: Response versus temperature curves of Pt/ZnO/ZnO, Pd-Ag (26%)/ZnO/Zn, and Rh/ZnO/Zn MIM sensors in the presence of 1% methane in (a) pure nitrogen and in (b) synthetic air.

competitive equilibrium between oxygen and hydrogen as the adsorbates on ZnO. As a result it may well be depicted that the adsorption sites for hydrogen are reduced and chemisorbed hydrogen reacts with oxygen instead of getting diffused into the noble metal/ZnO junction to produce H_2O molecules and thus reduce the current through the electrodes [126, 127]. Therefore, a lower response to hydrogen is obtained in synthetic air. The reactivity depends on the catalytic properties of the metal surface and differs between different metals. Since the OH formation energy barrier is much lower on Pt than Pd-Ag, most of the hydrogen produced by the dissociation of methane produces OH molecule for Pt contact. Then the water formation needs more than one step and thus the kinetics of sensing becomes slower.

Therefore, the devices using Pt as catalytic metal exhibit lower response and relatively longer response time than Pd-Ag for all the cases. The OH formation energy of Rh is higher than both Pd-Ag and Pt [128–131] and so Rh catalytic metal contact gives higher response than Pd-Ag and Pt. This corroborates the experimental results obtained by Bhattacharyya et al. [120].

Recently Bhattacharyya et al. [125] reported a ZnO-based resistive sensors with Au and Pd-Ag contact. The ZnO thin film was deposited by Sol-gel method. The crystal size of the films was in the range 45 nm–75 nm. The surface morphology studies revealed randomly oriented grains with hexagonal structure and a large number of

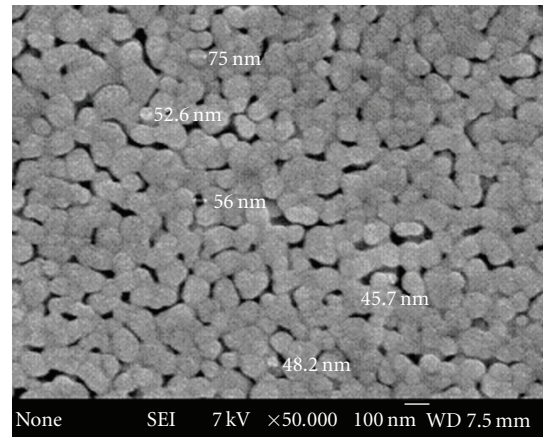

Figure 15: SEM images of the sol-gel grown nanocrystalline ZnO surface annealed at 600°C for 30 minutes.

pores of an average diameter 56 nm (Figure 15) that is very useful for methane gas sensing. It can be found that the operating temperature of sensing with Au contact was 350°C and it was reduced to 250°C (Figure 16) by using Pd-Ag catalytic contact with a response 74.3% and a response time ~16 seconds.

The same group reported a Pd-Ag/ZnO/Zn MIM methane sensor using sol-gel grown ZnO thin film, with

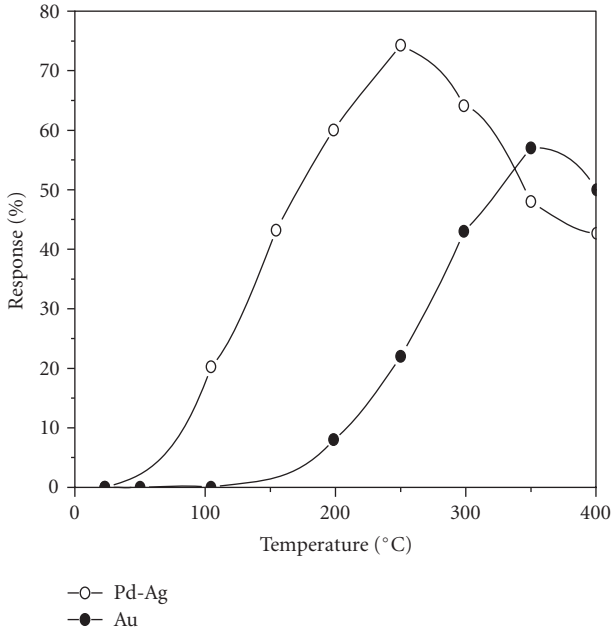

Figure 16: Response as a function of temperature.

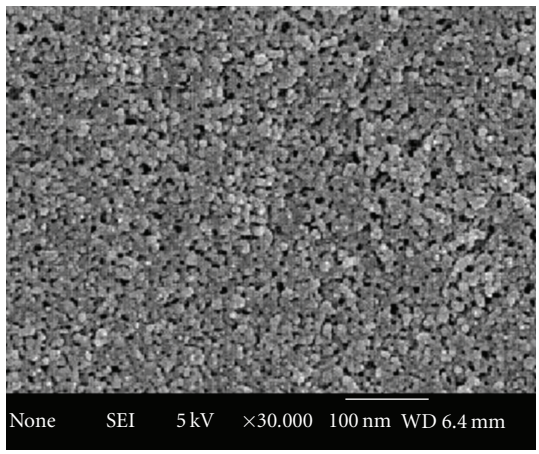

Figure 17: FESEM pictures of ZnO thin films grown electrochemically, with the magnification (× 30 000).

an operating temperature of 250°C and a response time ~11 seconds.

Basu [132] reduced the operating temperature of methane sensing to 100°C or less by using electrochemically grown nanocrystalline-nanoporous ZnO thin film and by modifying the oxide surface with Pd. Two different device configurations, for example, a planar structure and a metal-active insulator-metal (MIM) sandwich structure, both working on Schottky barrier mode were designed, fabricated, and tested for methane sensing. Pd-Ag alloy was used as the catalytic electrode (0.2 μm) contact for both the planar and MIM configurations.

Figure 17 shows the FESEM picture of the electrochemically grown nanocrystalline ZnO thin film. The crystallite size obtained was below 10 nm with a uniform distribution of the nanopores (size).

The variations of the response with operating temperature and with biasing voltage using 1% methane in nitrogen and in synthetic air were studied. The maximum response was obtained at 70°C and 100°C for the planar and the MIM sensor structures, respectively, with 3 V forward bias for both (Figures 18 and 19).

The Pd-modified nanocrystalline ZnO (below 10 nm) enhances the oxygen spillover process on ZnO matrix, resulting in a large amount of chemisorbed oxygen that yields a high electrostatic potential across the Pd-Ag/ZnO Schottky interface.

The change of current in presence of methane is relatively higher for the planar structure that has two Schottky contacts with double barriers compared to the MIM structure with one Pd-Ag/ZnO junction. The performance was somewhat reduced in synthetic air for both the sensor structures due to a competitive equilibrium between oxygen (from air) and hydrogen as the adsorbates on ZnO. As a result the adsorption sites for hydrogen and thus the amount of hydrogen diffusing across the Pd-Ag/ZnO junction are reduced. The temperature for maximum response was reduced to 70°C for the planar and 100°C for the MIM structures for the Pd-modified ZnO nanocrystals. The possible reason for the response at substantially low temperature was mentioned as due to increased surface free energy of the nanocrystalline ZnO surface. Presence of dispersed Pd nano particles over ZnO surface further reduces the adsorption energy. As a result the sensors respond at considerably low temperature and with short time of response. It is worth mentioning here that imperfect structural orientation of the polycrystalline sensing layer (ZnO) also modulates the gas adsorption behavior and thus the sensing parameters.

Figure 20 demonstrates that the sensors using Pd modified ZnO thin films show temperature dependent selectivity for methane and hydrogen in presence of each other. For the planar sensors hydrogen response is maximum at 50°C where the response for methane is very low. At 70°C both hydrogen and methanerespond almost to the same extent. On the other hand, MIM sensors show distinct selectivity for methane at 100°C where hydrogen response is almost zero.

Methane actually first dissociates to produce molecular hydrogen that subsequently decomposes catalytically to atomic hydrogen. The atomic hydrogen then takes part in gas sensing reaction. Therefore, the temperature for sensing methane is always higher than that of hydrogen.

The response time and recovery time were calculated from the transient response curves for different concentrations of methane and are shown in Table 1 .

Table 1 shows that the response and recovery times of the MIM sensor are relatively shorter than the planar sensor. The possible interpretation has been given that the separation between two electrodes for the planar configuration is larger (2 mm) than the MIM (8 μm) configuration, resulting in the rapid current flow kinetics for the MIM configuration.

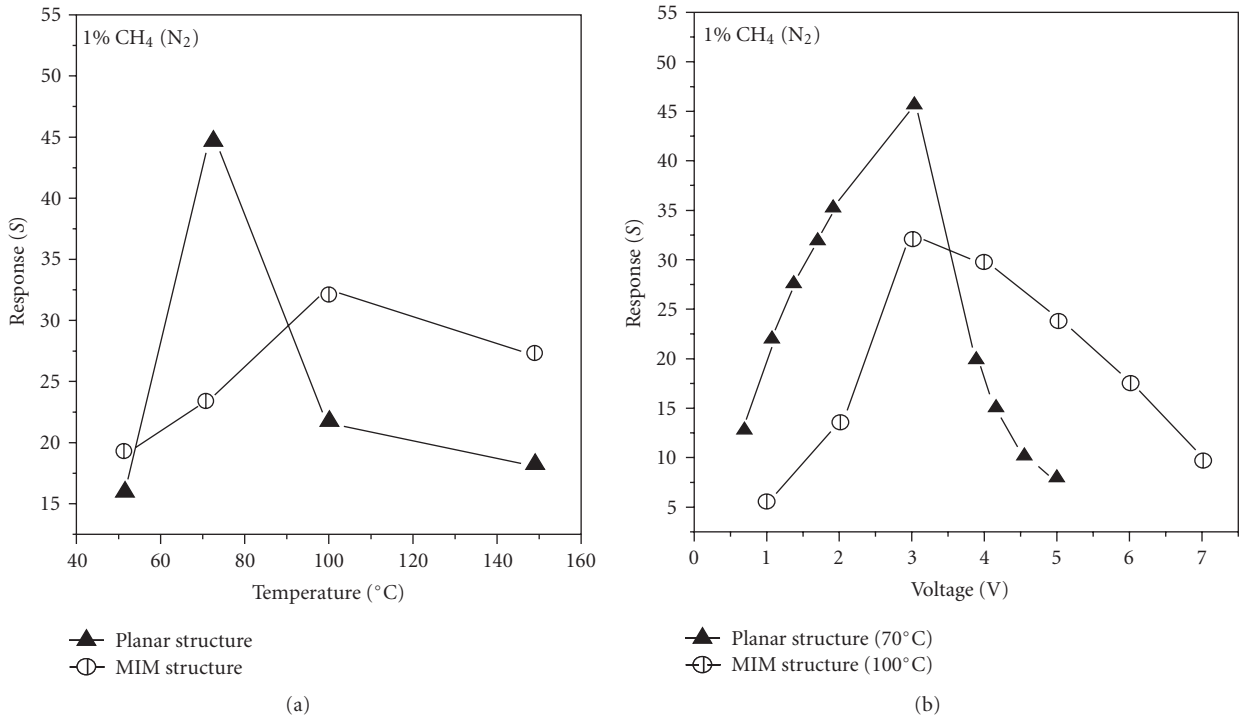

Figure 18: (a) Response versus temperature curves at 3 V and (b) response versus voltage curves, for planar and MIM sensor structures at 70°C and 100°C.

Table 1: The sensing results of the planar structures at 70°C and MIM structures at 100°C for different concentrations of methane using nitrogen and synthetic air as carrier gases.

% CH_4	Response				Response time (s)				Recovery time (s)			
	Planar		MIM		Planar		MIM		Planar		MIM	
	Nitrogen	Synthetic air	Nitrogen	Synthetic air	Nitrogen	Synthetic air	Nitrogen	Synthetic air	Nitrogen	Synthetic air	Nitrogen	Synthetic air
0.01	21.2	9.2	18.2	6.5	16.2	19.2	10.2	13.2	33.2	34.2	18.7	20.3
0.05	25.4	14.6	22.3	11.4	13.3	17.4	6.7	9.3	30.3	32.8	17.2	19.2
0.1	39.3	18.3	23.2	16.8	11.1	16.4	6.03	8.2	27.5	29.6	16.8	17.3
0.5	42.2	21.6	25.2	17.2	8.4	15.2	4.02	6.9	25.7	27.4	16.1	17.1
1	47.5	25.7	32.2	20.4	4.6	12.6	2.69	4.2	22.7	23.4	16.0	16.2

The longer time of recovery was due to slower rate of desorption being interfered by the presence of air after the methane flow was cut off.

This investigation highlights the fact that the temperature of sensing methane at 100°C using Pd-Ag/Pd: ZnO/Zn MIM device configuration is suitable for practical applications as due to minimum interference from humidity.

There are very few reports on metal oxide-based methane gas sensors with high response and shorter response and recovery time. So far the reported sensor structures based on oxide semiconductors and operating in the resistive mode at high temperature showed relatively longer response (>10 seconds) and recovery (>40 seconds) time for methane sensing. In this investigation, particularly the MIM sensor showed good response (~32), shorter response (~2.69 seconds), and recovery (~16 seconds) times as compared to the values reported by others [1–7, 91–105, 118–127, 133, 134].

Figure 21 presents the stability of both types of sensor structures. For 1% methane in nitrogen as carrier gas the study was continued for 33 days and showed a stable performance. In synthetic air the stability studied for about 9 hours was appreciably good.

5.3. Other Metal Oxide-Based Methane Gas Sensors. Apart from the ZnO-and SnO_2-based gas sensors, there are few metal oxides that give response towards the me-thane.

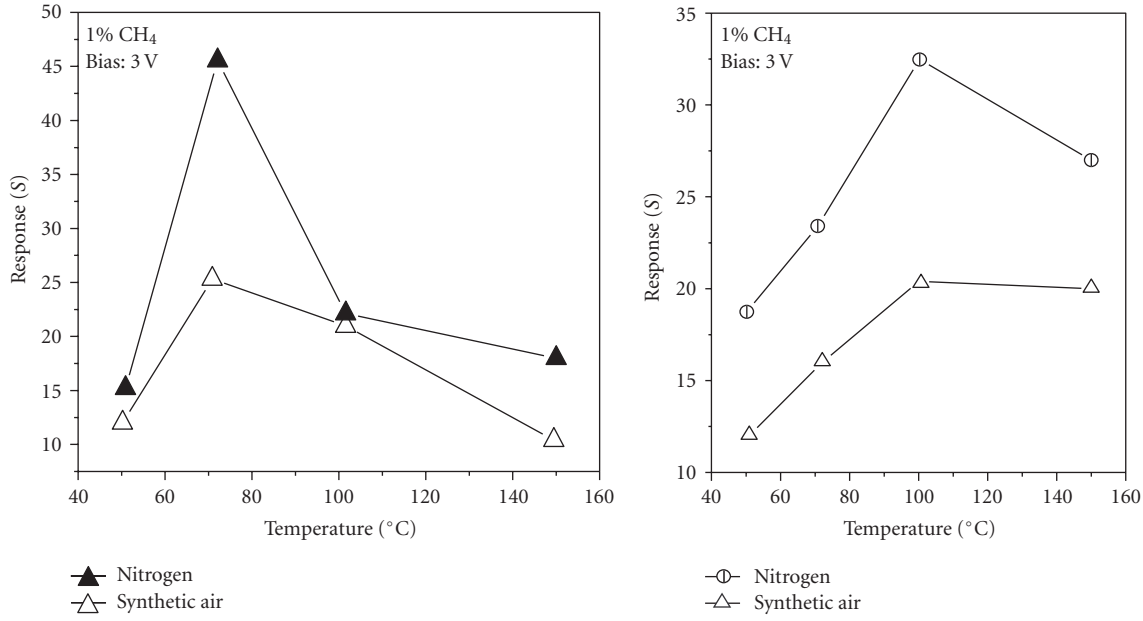

Figure 19: Response versus temperature curves of (a) the planar and (b) the MIM sensor structures at 3 V in the presence of 1% methane in pure nitrogen and in synthetic air.

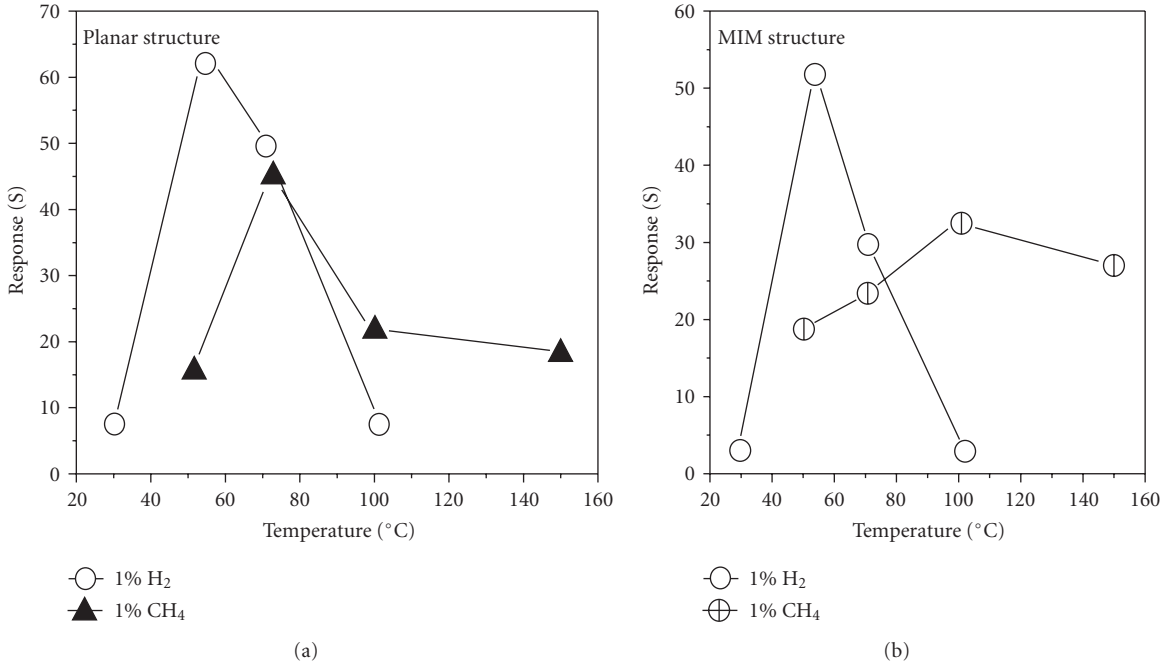

Figure 20: Response versus temperature plots of (a) the planar and (b) the MIM sensors in 1% H_2 and 1% CH_4 in pure N_2 environment.

Selective detection of methane in domestic environments using a catalyst sensor system based on Ga_2O_3 was reported by Flingelli et al. [133], and it was found that the use of catalytic gas filters consisting of porous Ga_2O_3 is very efficient to eliminate cross sensitivities to ethanol and organic solvents. This technique yields selective sensors for indoor methane detection and this type of catalyst filter is very promising in term of robustness. Moreover, no expensive catalytic material like platinum is required. Recently, MoO3-based CH_4 sensors were also reported [134]. However, the

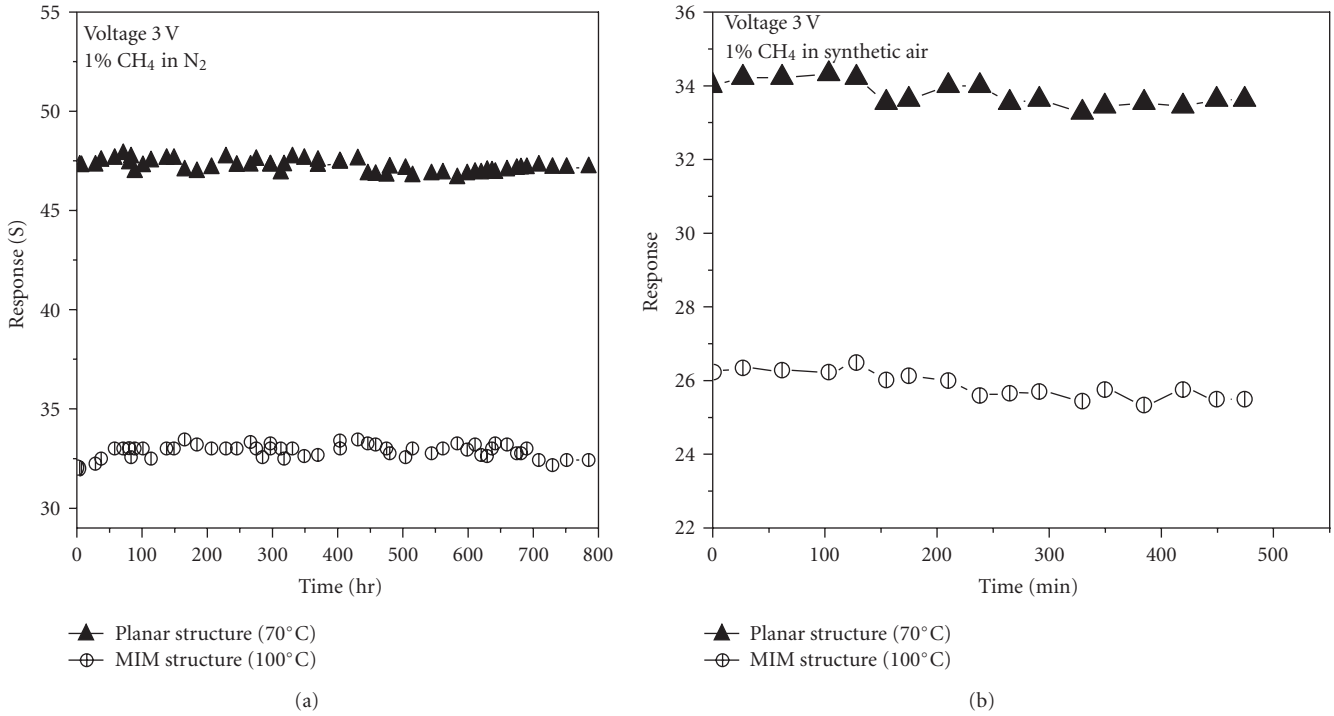

Figure 21: Stability study of both types of sensor structures using nitrogen as carrier gases.

sensor was operated at 500°C and the sensitivity for methane was quite poor.

6. Conclusion

This review article has focused on the recent achievement on the research and development of methane gas sensors using inexpensive metal oxides and the effect of noble metals, either as catalytic contact electrodes or as the sensitizing agents. Among them SnO_2 and ZnO sensors have been widely studied and have shown most promising results on gas response in terms of sensing temperature and voltage, sensitivity, time of response and stability. Nanocrystalline ZnO, after sensitization with Pd nanoparticles has shown the lowest temperature of methane sensing so far reported. Gas sensing mechanism has been briefly discussed from the point of view adsorption-desorption activation and the influence of noble metals.

Acknowledgments

The authors thankfully acknowledge the help and cooperation of Prof. H. Saha, Coordinator, and IC Design & Fabrication Centre, Department of Electronics & Telecommunication Engineering. Jadavpur University, Kolkata, for kindly providing the laboratory facilities. Thanks are also due to Dr. P. Bhattacharya, Ms. N. Saha, and Mr. S. K. Jana of the gas sensor group. P. K. Basu acknowledges CSIR, Government. of India, for kindly providing a Senior Research Fellowship (SRF).

References

[1] M. Fleischer and H. Meixner, "A selective CH_4 sensor using semiconducting Ga_2O_3 thin films based on temperature switching of multigas reactions," *Sensors and Actuators B*, vol. 25, no. 1–3, pp. 544–547, 1995.

[2] J. Wöllenstein, M. Burgmair, G. Plescher, et al., "Cobalt oxide based gas sensors on silicon substrate for operation at low temperatures," *Sensors and Actuators B*, vol. 93, no. 1–3, pp. 442–448, 2003.

[3] J. B. W. H. Brattain, "Surface properties of germanium," *Bell System Technical Journal*, vol. 32, 1952.

[4] D. M. Wilson, S. Hoyt, J. Janata, K. Booksh, and L. Obando, "Chemical sensors for portable, handheld field instruments," *IEEE Sensors Journal*, vol. 1, no. 4, pp. 256–274, 2001.

[5] J. Xu, Q. Pan, Y. Shun, and Z. Tian, "Grain size control and gas sensing properties of ZnO gas sensor," *Sensors and Actuators B*, vol. 66, no. 1, pp. 277–279, 2000.

[6] A. Trinchi, S. Kaciulis, L. Pandolfi, et al., "Characterization of Ga_2O_3 based MRISiC hydrogen gas sensors," *Sensors and Actuators B*, vol. 103, no. 1-2, pp. 129–135, 2004.

[7] X. Chen, W. Lu, W. Zhu, S. Y. Lim, and S. A. Akbar, "Structural and thermal analyses on phase evolution of sol-gel (Ba,Sr)TiO_3 thin films," *Surface and Coatings Technology*, vol. 167, no. 2-3, pp. 203–206, 2003.

[8] E. Comini, M. Ferroni, V. Guidi, G. Faglia, G. Martinelli, and G. Sberveglieri, "Nanostructured mixed oxides compounds for gas sensing applications," *Sensors and Actuators B*, vol. 84, no. 1, pp. 26–32, 2002.

[9] M. Rumyantseva, V. Kovalenko, A. Gaskov, et al., "Nanocomposites SnO_2/Fe_2O_3: sensor and catalytic properties," *Sensors and Actuators B*, vol. 118, no. 1-2, pp. 208–214, 2006.

[10] T. Islam and H. Saha, "Hysteresis compensation of a porous silicon relative humidity sensor using ANN technique," *Sensors and Actuators B*, vol. 114, no. 1, pp. 334–343, 2006.

[11] G. Kenanakis, D. Vernardou, E. Koudoumas, G. Kiriakidis, and N. Katsarakis, "Ozone sensing properties of ZnO nanostructures grown by the aqueous chemical growth technique," *Sensors and Actuators B*, vol. 124, no. 1, pp. 187–191, 2007.

[12] A. Teleki, S. E. Pratsinis, K. Kalyanasundaram, and P. I. Gouma, "Sensing of organic vapors by flame-made TiO_2 nanoparticles," *Sensors and Actuators B*, vol. 119, no. 2, pp. 683–690, 2006.

[13] J. Wöllenstein, M. Burgmair, G. Plescher, et al., "Cobalt oxide based gas sensors on silicon substrate for operation at low temperatures," *Sensors and Actuators B*, vol. 93, no. 1–3, pp. 442–448, 2003.

[14] A. Trinch, W. Wlodarski, Y. X. Li, G. Feglia, and G. Sberveglieri, "Pt,Ga_2O_3/SiC MRSiC devices: a study of the hydrogen response," *Journal of Physics D*, vol. 38, p. 754, 2005.

[15] L. Talazac, F. Barbarin, C. Varenne, L. Mazet, S. Pellier, and C. Soulier, "Gas sensing properties of pseudo-Schottky diodes on p-type indium phosphide substrates—application to O_3 and NO_2 monitoring in urban ambient air," *Sensors and Actuators B*, vol. 83, no. 1–3, pp. 149–159, 2002.

[16] K.-W. Lin, H.-I. Chen, C.-T. Lu, et al., "A hydrogen sensing Pd/InGaP metal-semiconductor (MS) Schottky diode hydrogen sensor," *Semiconductor Science and Technology*, vol. 18, no. 7, pp. 615–619, 2003.

[17] P. K. Basu, S. K. Jana, M. K. Mitra, H. Saha, and S. Basu, "Hydrogen gas sensors using anodically prepared and surface modified nanoporous ZnO thin films," *Sensor Letters*, vol. 6, no. 5, pp. 699–704, 2008.

[18] P. K. Basu, P. Bhattacharyya, N. Saha, H. Saha, and S. Basu, "Methane sensing properties of platinum catalysed nano porous zinc oxide thin films derived by electrochemical anodization," *Sensor Letters*, vol. 6, no. 1, pp. 219–225, 2008.

[19] M. Stamataki, D. Tsamakis, N. Brilis, I. Fasaki, A. Giannoudakos, and M. Kompitsas, "Hydrogen gas sensors based on PLD grown NiO thin film structures," *Physica Status Solidi*, vol. 205, no. 8, pp. 2064–2068, 2008.

[20] S. Basu and S. K. Hazra, "ZnO p-n homojunctions for hydrogen gas sensors at elevated temperature," *Asian Journal of Physics*, vol. 14, p. 65, 2005.

[21] S. K. Hazra and S. Basu, "Hydrogen sensitivity of ZnO p-n homojunctions," *Sensors and Actuators B*, vol. 117, no. 1, pp. 177–182, 2006.

[22] K.-K. Baek and H. L. Tuller, "Electronic characterization of ZnO/CuO heterojunctions," *Sensors and Actuators B*, vol. 13, no. 1–3, pp. 238–240, 1993.

[23] Y. Ushio, M. Miyayama, and H. Yanagida, "Effects of interface states on gas-sensing properties of a CuO/ZnO thin-film heterojunction," *Sensors and Actuators B*, vol. 17, no. 3, pp. 221–226, 1994.

[24] Y. Hu, X. Zhou, Q. Han, Q. Cao, and Y. Huang, "Sensing properties of CuO-ZnO heterojunction gas sensors," *Materials Science and Engineering B*, vol. 99, no. 1–3, pp. 41–43, 2003.

[25] Z. Ling, C. Leach, and R. Freer, "Heterojunction gas sensors for environmental NO_2 and CO_2 monitoring," *Journal of the European Ceramic Society*, vol. 21, no. 10-11, pp. 1977–1980, 2001.

[26] W.-Y. Chung, D.-D. Lee, and B.-K. Sohn, "Effects of added TiO_2 on the characteristics of SnO_2-based thick film gas sensors," *Thin Solid Films*, vol. 221, no. 1-2, pp. 304–310, 1992.

[27] K. Zakrzewska, M. Radecka, and M. Rekas, "Effect of Nb, Cr, Sn additions on gas sensing properties of TiO_2 thin films," *Thin Solid Films*, vol. 310, no. 1-2, pp. 161–166, 1997.

[28] M. Radecka, K. Zakrzewska, and M. Rekas, "SnO_2-TiO_2 solid solutions for gas sensors," *Sensors and Actuators B*, vol. 47, no. 1–3, pp. 194–204, 1998.

[29] V. Dusastre and D. E. Williams, "Gas-sensitive resistor properties of the solid solution series $Ti_x(Sn_{1-y}Sb_y)_{1-x}O_2$($0 < x < 1$, y = 0, 0.01, 0.05)," *Journal of Materials Chemistry*, vol. 9, no. 2, pp. 445–450, 1999.

[30] K. Zakrzewska, "Mixed oxides as gas sensors," *Thin Solid Films*, vol. 391, no. 2, pp. 229–238, 2001.

[31] J. L. Solis and V. Lantto, "A study of gas-sensing properties of sputtered α-$SnWO_4$ thin films," *Sensors and Actuators B*, vol. 25, no. 1–3, pp. 591–595, 1995.

[32] J. L. Solis and V. Lantto, "Gas-sensing properties of different α-$SnWO_4$-based thick films," *Physica Scripta T*, vol. 69, pp. 281–285, 1997.

[33] P. Nelli, L. E. Depero, M. Ferroni, et al., "Sub-ppm NO_2 sensors based on nanosized thin films of titanium-tungsten oxides," *Sensors and Actuators B*, vol. 31, no. 1-2, pp. 89–92, 1996.

[34] L. E. Depero, M. Ferroni, V. Guidi, et al., "Preparation and micro-structural characterization of nanosized thin film of TiO_2-WO_3 as a novel material with high sensitivity towards NO_2," *Sensors and Actuators B*, vol. 36, no. 1–3, pp. 381–383, 1996.

[35] V. Guidi, M. C. Carotta, M. Ferroni, et al., "Preparation of nanosized titania thick and thin films as gas-sensors," *Sensors and Actuators B*, vol. 57, no. 1–3, pp. 197–200, 1999.

[36] E. Comini, M. Ferroni, V. Guidi, G. Faglia, G. Martinelli, and G. Sberveglieri, "Nanostructured mixed oxides compounds for gas sensing applications," *Sensors and Actuators B*, vol. 84, no. 1, pp. 26–32, 2002.

[37] P. Bhattacharyya, P. K. Basu, C. Lang, H. Saha, and S. Basu, "Noble metal catalytic contacts to sol-gel nanocrystalline zinc oxide thin films for sensing methane," *Sensors and Actuators B*, vol. 129, no. 2, pp. 551–557, 2008.

[38] H.-W. Cheong and M.-J. Lee, "Sensing characteristics and surface reaction mechanism of alcohol sensors based on doped SnO_2," *Journal of Ceramic Processing Research*, vol. 7, no. 3, pp. 183–191, 2006.

[39] L. Castañeda, "Effects of palladium coatings on oxygen sensors of titanium dioxide thin films," *Materials Science and Engineering B*, vol. 139, no. 2-3, pp. 149–154, 2007.

[40] V. R. Shinde, T. P. Gujar, and C. D. Lokhande, "Enhanced response of porous ZnO nanobeads towards LPG: effect of Pd sensitization," *Sensors and Actuators B*, vol. 123, no. 2, pp. 701–706, 2007.

[41] S. W. Hla, P. Lacovig, G. Comelli, A. Baraldi, M. Kiskinova, and R. Rosei, "Orientational anisotropy in oxygen dissociation on Rh(110)," *Physical Review B*, vol. 60, no. 11, pp. 7800–7803, 1999.

[42] A. Rothschild and Y. Komem, "The effect of grain size on the sensitivity of nanocrystalline metal-oxide gas sensors," *Journal of Applied Physics*, vol. 95, no. 11, pp. 6374–6380, 2004.

[43] S. L. Tait, Z. Dohnálek, C. T. Campbell, and B. D. Kay, "Methane adsorption and dissociation and oxygen adsorption and reaction with CO on Pd nanoparticles on MgO(1 0 0) and on Pd(1 1 1)," *Surface Science*, vol. 591, no. 1–3, pp. 90–107, 2005.

[44] M. Ali, V. Cimalla, V. Lebedev, et al., "Pt/GaN Schottky diodes for hydrogen gas sensors," *Sensors and Actuators B*, vol. 113, no. 2, pp. 797–804, 2006.

[45] C. Xu, J. Tamaki, N. Miura, and N. Yamazoe, "Relationship between gas sensitivity and microstructure of porous SnO_2," *Journal of The Electrochemical Society*, vol. 58, p. 1143, 1990.

[46] H. Zhang, R. L. Penn, R. J. Hamers, and J. F. Banfield, "Enhanced adsorption of molecules on surfaces of nanocrystalline particles," *Journal of Physical Chemistry B*, vol. 103, no. 22, pp. 4656–4662, 1999.

[47] C. Xu, J. Tamaki, N. Miura, and N. Yamazoe, "Grain size effects on gas sensitivity of porous SnO_2-based elements," *Sensors and Actuators B*, vol. 3, no. 2, pp. 147–155, 1991.

[48] M. Tiemann, "Porous metal oxides as gas sensors," *Chemistry*, vol. 13, no. 30, pp. 8376–8388, 2007.

[49] G. Sakai, N. S. Baik, N. Miura, and N. Yamazoe, "Gas sensing properties of tin oxide thin films fabricated from hydrothermally treated nanoparticles: dependence of CO and H_2 response on film thickness," *Sensors and Actuators B*, vol. 77, no. 1-2, pp. 116–121, 2001.

[50] P. K. Basu, P. Bhattacharyya, N. Saha, H. Saha, and S. Basu, "The superior performance of the electrochemically grown ZnO thin films as methane sensor," *Sensors and Actuators B*, vol. 133, no. 2, pp. 357–363, 2008.

[51] G. Korotcenkov, V. Brinzari, J. Schwank, M. DiBattista, and A. Vasiliev, "Peculiarities of SnO_2 thin film deposition by spray pyrolysis for gas sensor application," *Sensors and Actuators B*, vol. 77, no. 1-2, pp. 244–252, 2001.

[52] G. Sakai, N. Matsunaga, K. Shimanoe, and N. Yamazoe, "Theory of gas-diffusion controlled sensitivity for thin film semiconductor gas sensor," *Sensors and Actuators B*, vol. 80, no. 2, pp. 125–131, 2001.

[53] F. Hossein-Babaei and M. Orvatinia, "Analysis of thickness dependence of the sensitivity in thin film resistive gas sensors," *Sensors and Actuators B*, vol. 89, no. 3, pp. 256–261, 2003.

[54] D. Ding, Z. Chen, and C. Lu, "Hydrogen sensing of nanoporous palladium films supported by anodic aluminum oxides," *Sensors and Actuators B*, vol. 120, no. 1, pp. 182–186, 2006.

[55] I. Lundstrom, H. Sundgren, F. Winquist, M. Eriksson, C. Krantz-Rulcker, and A. Lloyd-Spetz, "Twenty-five years of field effect gas sensor research in Linkoping," *Sensors and Actuators B*, vol. 121, no. 1, pp. 247–262, 2007.

[56] M. Lofdahl, C. Utaiwasin, A. Carlsson, I. Lundstrom, and M. Eriksson, "Gas response dependence on gate metal morphology of field-effect devices," *Sensors and Actuators B*, vol. 80, no. 3, pp. 183–192, 2001.

[57] M. Armgarth and C. Nylander, "Blister formation in Pd gate MIS hydrogen sensors," *IEEE Electron Device Letters*, vol. 3, no. 12, pp. 384–386, 1982.

[58] S. C. Su, J. N. Carstens, and A. T. Bell, "A study of the dynamics of Pd oxidation and PdO reduction by H_2 and CH_4," *Journal of Catalysis*, vol. 176, no. 1, pp. 125–135, 1998.

[59] M. Wang and Y. Feng, "Palladium-silver thin film for hydrogen sensing," *Sensors and Actuators B*, vol. 123, no. 1, pp. 101–106, 2007.

[60] R. C. Hughes, W. K. Schubert, T. E. Zipperian, J. L. Rodriguez, and T. A. Plut, "Thin film palladium and shiver alloys and layers for metal-insulator-semiconductor sensors," *Journal of Applied Physics*, vol. 62, p. 1074, 1987.

[61] V. A. Drozdov, P. G. Tsyrulnikov, V. V. Popovskii, N. N. Bulgakov, E. M. Moroz, and T. G. Galeev, "Comparative study of the activity of Al-Pd and Al-Pt catalysts in deep oxidation of hydrocarbons," *Reaction Kinetics and Catalysis Letters*, vol. 27, no. 2, pp. 425–427, 1985.

[62] B. L. Zhu, C. S. Xie, D. W. Zeng, W. L. Song, and A. M. Wang, "Investigation of gas sensitivity of Sb-doped ZnO nanoparticles," *Materials Chemistry and Physics*, vol. 89, no. 1, pp. 148–153, 2005.

[63] M. N. Rumyantseva, V. V. Kovalenko, A. M. Gas'kov, and T. Pagnier, "Metal-oxide based nanocomposites as materials for gas sensors," *Russian Journal of General Chemistry*, vol. 78, no. 5, pp. 1081–1092, 2008.

[64] F. Volkenshtein, *Electronic Theory of Catalysis on Semiconductors*, Fizmatgiz, Moscow, Russia, 1960.

[65] G. Korotcenkov, "Gas response control through structural and chemical modification of metal oxide films: state of the art and approaches," *Sensors and Actuators B*, vol. 107, no. 1, pp. 209–232, 2005.

[66] J. F. McAleer, P. T. Moseley, J. O. W. Norris, D. E. Williams, and B. C. Tofield, "Tin dioxide gas sensors—part 2: the role of surface additives," *Journal of the Chemical Society, Faraday Transactions 1*, vol. 84, no. 2, pp. 441–457, 1988.

[67] V. Brinzari, G. Korotcenkov, J. Schwank, and Y. Boris, "Chemisorptionoal approach to kinetic analysis of SnO_2:Pd-based thin film gas sensors (TFGS)," *Journal of Optoelectronics and Advanced Materials*, vol. 4, no. 1, p. 147, 2002.

[68] G. Korotcenkov, V. Brinzari, Y. Boris, M. Ivanov, J. Schwank, and J. Morante, "Influence of surface Pd doping on gas sensing characteristics of SnO_2 thin films deposited by spray pirolysis," *Thin Solid Films*, vol. 436, no. 1, pp. 119–126, 2003.

[69] V. R. Shinde, T. P. Gujar, and C. D. Lokhande, "Enhanced response of porous ZnO nanobeads towards LPG: effect of Pd sensitization," *Sensors and Actuators B*, vol. 123, no. 2, pp. 701–706, 2007.

[70] W. Göpel and K. D. Schierbaum, "SnO_2 sensors: current status and future prospects," *Sensors and Actuators B*, vol. 26, no. 1–3, pp. 1–12, 1995.

[71] M. J. Madou and S. R. Morrison, *Chemical Sensing with Solid-State Devices*, Academic Press, New York, NY, USA, 1989.

[72] J.-H. Sung, Y.-S. Lee, J.-W. Lim, Y.-H. Hong, and D.-D. Lee, "Sensing characteristics of tin dioxide/gold sensor prepared by coprecipitation method," *Sensors and Actuators B*, vol. 66, no. 1, pp. 149–152, 2000.

[73] K. L. Chopra, S. Major, and D. K. Pandya, "Transparent conductors—a status review," *Thin Solid Films*, vol. 102, no. 1, pp. 1–46, 1983.

[74] T. W. Kim, D. U. Lee, J. H. Lee, D. C. Choo, M. Jung, and Y. S. Yoon, "Structural, electrical, and optical properties of SnO_2 nanocrystalline thin films grown on *p*-InSb (111) substrates," *Journal of Applied Physics*, vol. 90, no. 1, pp. 175–180, 2001.

[75] G. G. Mandayo, E. Castano, F. J. Gracia, A. Cirera, A. Cornet, and J. R. Morante, "Strategies to enhance the carbon monoxide sensitivity of tin oxide thin films," *Sensors and Actuators B*, vol. 95, no. 1–3, pp. 90–96, 2003.

[76] H. Ogawa, M. Nishikawa, and A. Abe, "Hall measurement studies and an electrical conduction model of tin oxide ultrafine particle films," *Journal of Applied Physics*, vol. 53, no. 6, pp. 4448–4455, 1982.

[77] V. R. Katti, A. K. Debnath, K. P. Muthe, et al., "Mechanism of drifts in H_2S sensing properties of SnO_2:CuO composite thin

film sensors prepared by thermal evaporation," *Sensors and Actuators B*, vol. 96, no. 1-2, pp. 245–252, 2003.

[78] B.-K. Min and S.-D. Choi, "SnO_2 thin film gas sensor fabricated by ion beam deposition," *Sensors and Actuators B*, vol. 98, no. 2-3, pp. 239–246, 2004.

[79] G. Korotcenkov, V. Brinzari, V. Golovanov, and Y. Blinov, "Kinetics of gas response to reducing gases of SnO_2 films, deposited by spray pyrolysis," *Sensors and Actuators B*, vol. 98, no. 1, pp. 41–45, 2004.

[80] S. Shukla, S. Patil, S. C. Kuiry, et al., "Synthesis and characterization of sol-gel derived nanocrystalline tin oxide thin film as hydrogen sensor," *Sensors and Actuators B*, vol. 96, no. 1-2, pp. 343–353, 2003.

[81] G. Sberveglieri, "Classical and novel techniques for the preparation of SnO_2 thin-film gas sensors," *Sensors and Actuators B*, vol. 6, no. 1–3, pp. 239–247, 1992.

[82] R. Dolbec, M. A. El Khakani, A. M. Serventi, and R. G. Saint-Jacques, "Influence of the nanostructural characteristics on the gas sensing properties of pulsed laser deposited tin oxide thin films," *Sensors and Actuators B*, vol. 93, no. 1–3, pp. 566–571, 2003.

[83] D. B. Chrisey and G. K. Hubler, Eds., *Pulsed Laser Deposition of Thin Films*, John Wiley & Sons, New York, NY, USA, 1994.

[84] M. C. Carotta, V. Guidi, G. Martinelli, M. Nagliati, D. Puzzovio, and D. Vecchi, "Sensing of volatile alkanes by metal-oxide semiconductors," *Sensors and Actuators B*, vol. 130, no. 1, pp. 497–501, 2008.

[85] H. H. Kung, "Oxidative dehydrogenation of light (C2 to C4) alkanes," *Advanced Catalyst*, vol. 40, p. 1, 1994.

[86] I.-C. Marcu, J.-M. M. Millet, and J.-M. Herrmann, "Semiconductive and redox properties of Ti and Zr pyrophosphate catalysts (TiP_2O_7 and ZrP_2O_7). Consequences for the oxidative dehydrogenation of *n*-butane," *Catalysis Letters*, vol. 78, no. 1–4, pp. 273–279, 2002.

[87] I.-C. Marcu, J.-M. M. Millet, and I. Săndulescu, "Oxidative dehydrogenation of isobutane over a titanium pyrophosphate catalyst," *Journal of the Serbian Chemical Society*, vol. 70, no. 6, pp. 791–798, 2005.

[88] M. C. Carotta, A. Cervi, A. Giberti, et al., "Ethanol interference in light alkane sensing by metal-oxide solid solutions," *Sensors and Actuators B*, vol. 136, no. 2, pp. 405–409, 2009.

[89] M. C. Carotta, A. Cervi, A. Giberti, et al., "Metal-oxide solid solutions for light alkane sensing," *Sensors and Actuators B*, vol. 133, no. 2, pp. 516–520, 2008.

[90] M. C. Carotta, V. Guidi, G. Martinelli, M. Nagliati, D. Puzzovio, and D. Vecchi, "Sensing of volatile alkanes by metal-oxide semiconductors," *Sensors and Actuators B*, vol. 130, no. 1, pp. 497–501, 2008.

[91] M. V. Vaishampayan, R. G. Deshmukh, and I. S. Mulla, "Influence of Pd doping on morphology and LPG response of SnO_2," *Sensors and Actuators B*, vol. 131, no. 2, pp. 665–672, 2008.

[92] A. Cabot, A. Vilà, and J. R. Morante, "Analysis of the catalytic activity and electrical characteristics of different modified SnO_2 layers for gas sensors," *Sensors and Actuators B*, vol. 84, no. 1, pp. 12–20, 2002.

[93] N. Das, A. K. Halder, J. M. A. Sen, and H. S. Maiti, "Sonochemically prepared tin-dioxide based composition for methane sensor," *Materials Letters*, vol. 60, no. 8, pp. 991–994, 2006.

[94] B.-K. Min and S.-D. Choi, "Undoped and 0.1 wt.% Ca-doped Pt-catalyzed SnO_2 sensors for CH_4 detection," *Sensors and Actuators B*, vol. 108, no. 1-2, pp. 119–124, 2005.

[95] S. Bose, S. Chakraborty, B. K. Ghosh, D. Das, A. Sen, and H. S. Maiti, "Methane sensitivity of Fe-doped SnO_2 thick films," *Sensors and Actuators B*, vol. 105, no. 2, pp. 346–350, 2005.

[96] F. Quaranta, R. Rella, P. Siciliano, et al., "Novel gas sensor based on SnO_2/Os thin film for the detection of methane at low temperature," *Sensors and Actuators B*, vol. 58, no. 1–3, pp. 350–355, 1999.

[97] K. Chatterjee, S. Chatterjee, A. Banerjee, et al., "The effect of palladium incorporation on methane sensitivity of antimony doped tin dioxide," *Materials Chemistry and Physics*, vol. 81, no. 1, pp. 33–38, 2003.

[98] J. C. Kim, H. K. Jun, J.-S. Huh, and D. D. Lee, "Tin oxide-based methane gas sensor promoted by alumina-supported Pd catalyst," *Sensors and Actuators B*, vol. 45, no. 3, pp. 271–277, 1997.

[99] L. Urfels, P. Gelin, M. Primet, and E. Tena, "Complete oxidation of methane at low temperature over Pt catalysts supported on high surface area SnO_2," *Topics in Catalysis*, vol. 30-31, pp. 427–432, 2004.

[100] C. K. Kim, J. H. Lee, S. M. Choi, et al., "Pd- and Pt-SiC Schottky diodes for detection of H_2 and CH_4 at high temperature," *Sensors and Actuators B*, vol. 77, no. 1-2, pp. 455–462, 2001.

[101] S. Chakraborty, A. Sen, and H. S. Maiti, "Complex plane impedance plot as a figure of merit for tin dioxide-based methane sensors," *Sensors and Actuators B*, vol. 119, no. 2, pp. 431–434, 2006.

[102] K. R. Han, C.-S. Kim, K. T. Kang, H. J. Koo, D. Kang II, and J. He, "Development of SnO_2 based semiconductor gas sensor with Fe_2O_3 for detection of combustible gas," *Journal of Electroceramics*, vol. 10, no. 1, pp. 69–73, 2003.

[103] V. V. Malyshev and A. V. Pislyakov, "Dynamic properties and sensitivity of semiconductor metal-oxide thick-film sensors to various gases in air gaseous medium," *Sensors and Actuators B*, vol. 96, no. 1-2, pp. 413–434, 2003.

[104] M. Saha, A. Banerjee, A. K. Halder, J. Mondal, A. Sen, and H. S. Maiti, "Effect of alumina addition on methane sensitivity of tin dioxide thick films," *Sensors and Actuators B*, vol. 79, no. 2-3, pp. 192–195, 2001.

[105] A. Chen, S. Bai, B. Shi, Z. Liu, D. Li, and C. C. Liu, "Methane gas-sensing and catalytic oxidation activity of SnO_2-In_2O_3 nanocomposites incorporating TiO_2," *Sensors and Actuators B*, vol. 135, no. 1, pp. 7–12, 2008.

[106] X. L. Cheng, H. Zhao, L. H. Huo, S. Gao, and J. G. Zhao, "ZnO nanoparticulate thin film: preparation, characterization and gas-sensing property," *Sensors and Actuators B*, vol. 102, no. 2, pp. 248–252, 2004.

[107] M. Suchea, S. Christoulakis, K. Moschovis, N. Katsarakis, and G. Kiriakidis, "ZnO transparent thin films for gas sensor applications," *Thin Solid Films*, vol. 515, no. 2, pp. 551–554, 2006.

[108] G. Eranna, B. C. Joshi, D. P. Runthala, and R. P. Gupta, "Oxide materials for development of integrated gas sensors–a comprehensive review," *Critical Reviews in Solid State and Materials Sciences*, vol. 29, no. 3-4, pp. 111–188, 2004.

[109] S. Cho, J. Ma, Y. Kim, Y. Sun, G. K. L. Wong, and J. B. Ketterson, "Photoluminescence and ultraviolet lasing of polycrystalline ZnO thin films prepared by the oxidation of the metallic Zn," *Applied Physics Letters*, vol. 75, no. 18, pp. 2761–2763, 1999.

[110] R. Bel Hadj Tahar, "Structural and electrical properties of aluminum-doped zinc oxide films prepared by sol-gel process," *Journal of the European Ceramic Society*, vol. 25, no. 14, pp. 3301–3306, 2005.

[111] A. Ashida, T. Nagata, and N. Fujimura, "Electro-optical effect in ZnO:Mn thin films prepared by Xe sputtering," *Journal of Applied Physics*, vol. 99, no. 1, Article ID 013509, 4 pages, 2006.

[112] S. Muthukumar, C. R. Gorla, N. W. Emanetoglu, S. Liang, and Y. Lu, "Control of morphology and orientation of ZnO thin films grown on SiO_2/Si substrates," *Journal of Crystal Growth*, vol. 225, no. 2–4, pp. 197–201, 2001.

[113] J. F. Muth, R. M. Kolbas, A. K. Sharma, S. Oktyabrsky, and J. Narayan, "Excitonic structure and absorption coefficient measurements of ZnO single crystal epitaxial films deposited by pulsed laser deposition," *Journal of Applied Physics*, vol. 85, no. 11, pp. 7884–7887, 1999.

[114] M. Jin, J. Feng, Z. De-Heng, M. Hong-Lei, and L. Shu-Ying, "Optical and electronic properties of transparent conducting ZnO and ZnO:Al films prepared by evaporating method," *Thin Solid Films*, vol. 357, no. 2, pp. 98–101, 1999.

[115] H. Yan, Y. Yang, Z. Fu, et al., "Fabrication of 2D and 3D ordered porous ZnO films using 3D opal templates by electrodeposition," *Electrochemistry Communications*, vol. 7, no. 11, pp. 1117–1121, 2005.

[116] G. S. Wu, T. Xie, X. Y. Yuan, et al., "Controlled synthesis of ZnO nanowires or nanotubes via sol-gel template process," *Solid State Communications*, vol. 134, no. 7, pp. 485–489, 2005.

[117] P. Mitra and A. K. Mukhopadhyay, "ZnO thin film as methane sensor," *Bulletin of the Polish Academy of Sciences: Technical Sciences*, vol. 55, no. 3, pp. 281–285, 2007.

[118] P. Bhattacharyya, P. K. Basu, H. Saha, and S. Basu, "Fast response methane sensor based on Pd(Ag)/ZnO/Zn MIM structure," *Sensor Letters*, vol. 4, no. 4, pp. 371–376, 2006.

[119] P. Bhattacharyya, P. K. Basu, H. Saha, and S. Basu, "Fast response methane sensor using nanocrystalline zinc oxide thin films derived by sol-gel method," *Sensors and Actuators B*, vol. 124, no. 1, pp. 62–67, 2007.

[120] P. Bhattacharyya, P. K. Basu, C. Lang, H. Saha, and S. Basu, "Noble metal catalytic contacts to sol-gel nanocrystalline zinc oxide thin films for sensing methane," *Sensors and Actuators B*, vol. 129, no. 2, pp. 551–557, 2008.

[121] S. J. Fonash, J.-A. Roger, and C. H. S. Dupuy, "Ac equivalent circuits for MIM structures," *Journal of Applied Physics*, vol. 45, no. 7, pp. 2907–2910, 1974.

[122] S. Basu and A. Dutta, "Room-temperature hydrogen sensors based on ZnO," *Materials Chemistry and Physics*, vol. 47, no. 1, pp. 93–96, 1997.

[123] M. Fleischer and H. Meixner, "A selective CH_4 sensor using semiconducting Ga_2O_3 thin films based on temperature switching of multigas reactions," *Sensors and Actuators B*, vol. 25, no. 1–3, pp. 544–547, 1995.

[124] J. Wollllenstein, M. Burgmair, G. Plescher, et al., "Cobalt oxide based gas sensors on silicon substrate for operation at low temperatures," *Sensors and Actuators B*, vol. 93, no. 1–3, pp. 442–448, 2003.

[125] P. Bhattacharyya, P. K. Basu, H. Saha, and S. Basu, "Fast response methane sensor using nanocrystalline zinc oxide thin films derived by sol-gel method," *Sensors and Actuators B*, vol. 124, no. 1, pp. 62–67, 2007.

[126] P. K. Basu, P. Bhattacharyya, N. Saha, H. Saha, and S. Basu, "The superior performance of the electrochemically grown ZnO thin films as methane sensor," *Sensors and Actuators B*, vol. 133, no. 2, pp. 357–363, 2008.

[127] P. K. Basu, P. Bhattacharyya, N. Saha, H. Saha, and S. Basu, "Methane sensing properties of platinum catalysed nano porous zinc oxide thin films derived by electrochemical anodization," *Sensor Letters*, vol. 6, no. 1, pp. 219–225, 2008.

[128] R. Löber and D. Hennig, "Interaction of hydrogen with transition metal fcc(111) surfaces," *Physical Review B*, vol. 55, no. 7, pp. 4761–4765, 1997.

[129] E. P. J. Mallens, J. H. B. J. Hoebink, and G. B. Marin, "The reaction mechanism of the partial oxidation of methane to synthesis gas: a transient kinetic study over rhodium and a comparison with platinum," *Journal of Catalysis*, vol. 167, no. 1, pp. 43–56, 1997.

[130] L. Opara, B. Klein, and H. Züchner, "Hydrogen-diffusion in $Pd_{1-x}Ag_x (0 \leq x \leq 1)$," *Journal of Alloys and Compounds*, vol. 253-254, pp. 378–380, 1997.

[131] S. Eriksson, M. Nilsson, M. Boutonnet, and S. Järås, "Partial oxidation of methane over rhodium catalysts for power generation applications," *Catalysis Today*, vol. 100, no. 3-4, pp. 447–451, 2005.

[132] P. K. Basu, S. K. Jana, H. Saha, and S. Basu, "Low temperature methane sensing by electrochemically grown and surface modified ZnO thin films," *Sensors and Actuators B*, vol. 135, no. 1, pp. 81–88, 2008.

[133] G. K. Flingelli, M. M. Fleischer, and H. Meixner, "Selective detection of methane in domestic environments using a catalyst sensor system based on Ga_2O_3," *Sensors and Actuators B*, vol. 48, no. 1–3, pp. 258–262, 1998.

[134] S. Barazzouk, R. P. Tandon, and S. Hotchandani, "MoO_3-based sensor for NO, NO_2 and CH_4 detection," *Sensors and Actuators B*, vol. 119, no. 2, pp. 691–694, 2006.